Constitutive equations for ionic transport in porous shales

A. Revil and P. Leroy

Département d'Hydrogéophysique et Milieux Poreux, Centre Européen de Recherche et d'Enseignement de Géosciences de l'Environnement, Centre National de la Recherche Scientifique, Aix-en-Provence, France

Received 22 August 2003; revised 5 January 2004; accepted 14 January 2004; published 27 March 2004.

[1] The constitutive coupled equations describing ionic transport in a porous shale are obtained at the scale of a representative elementary volume by volume averaging the local Nernst-Planck and Stokes equations. The final relationships check the Onsager reciprocity to the first order of perturbation of the state variables with respect to the thermostatic state. This state is characterized by a modified version of the Donnan equilibrium model, which accounts for the partition of the counterions between the Stern and diffuse Gouy-Chapman layers. After upscaling the local equations the material properties entering the macroscopic constitutive equations are explicitly related to the porosity of the shale, its cation exchange capacity, and some textural properties such as the electrical cementation exponent entering Archie's law. This new model is then applied to predict the salt filtering and electrodiffusion efficiencies of a shale layer. *INDEX TERMS:* 0619 Electromagnetics: Electromagnetic theory; 5109 Physical Properties of Rocks: Magnetic and electrical properties; 5112 Physical Properties of Rocks: Microstructure; 5134 Physical Properties of Rocks: Thermal properties; 5139 Physical Properties of Rocks: Transport properties; *KEYWORDS:* diffusion, electrokinetic, shale

Citation: Revil, A., and P. Leroy (2004), Constitutive equations for ionic transport in porous shales, *J. Geophys. Res.*, *109*, B03208, doi:10.1029/2003JB002755.

1. Introduction

[2] The inherent difficulty in the study of ionic transport in shales concerns the modeling of the coupling effects between the various thermodynamic forces and fluxes existing in the open (permeable) thermodynamic system. In shales, most of the coupling phenomena arise from the intrinsic charge of clay minerals and their high specific surface areas. The excess charge of clays is the result of isomorphic substitutions inside their crystalline framework and of chemical speciations between their surface reactive groups (e.g., silanols and aluminols) and the ions in the pore water. The excess charge of the clay minerals is counterbalanced by charge carriers of opposite sign (the "counterions") located in the pore water. The resulting disturbances of the ionic concentrations are described by the "electrical triple layer" (TLM) model. In shales, the size of the diffuse (Gouy-Chapman) part of the triple layer can be on the same order of magnitude than the size of the throats controlling transport properties through the connected porosity. This is especially true when the ionic strength of the fluid in equilibrium with the shale is low (typically below 0.1 mol L^{-1}). So models based on the thin electrical diffuse layer assumption [e.g., *Pride*, 1994] are not valid in this situation. The whole pore water of a shale, and not only the fraction enclosed in the vicinity of the mineral surface, does not follow the electroneutrality condition. In other words, the electroneutrality condition in the pore water must be modified to include the excess charge of the clay minerals.

[3] There is a considerable number of works in the literature dedicated to modeling coupled transport of ions through charged porous materials. For example, *Kedem and Katchalsky* [1961] and *Michaeli and Kedem* [1961] postulated equations coupling current density, diffusion flux, and solvent flux to their associated thermodynamic forces, namely the electrical field, the gradient of chemical potential of the brine, and the fluid pressure gradient. Their model is based on thermodynamic arguments of irreversible linear thermodynamics. However, this was mainly a phenomenological theory in which the material properties were not specified as functions of the constituent properties and microstructural parameters.

[4] To our knowledge, there has been no attempt yet to model the coupling between the four thermodynamic fluxes of interest in shales (e.g., ionic fluxes, current density, solvent flux, and heat flow), explicitly based on the underlying constituent properties and excluding the thin electrical diffuse layer assumption. In this paper, the continuum equations known to apply to the ions, the solvent (water), and solid phase at the local scale are volume averaged to obtain the macroscopic equations at the scale of a representative elementary volume of the porous shale considered as a granular charged porous material. The Onsager reciprocity, valid at the macroscopic scale, is consistent with a linearization of the local constitutive equations.

[5] To keep our theory as simple as possible, we make the following assumptions.

0148-0227/04/2003JB002755$09.00

Table 1. Properties of the Brine, Pore Water, and Ions

Property	Meaning	Unit
$C_f(C_f^0)$	salinity of the brine in the reservoirs	m^{-3}
C_w (C_w^0)	concentration of water in the reservoirs	m^{-3}
$\overline{C}_w(\overline{C}_w^0)$	concentration of water in the shale	m^{-3}
$C_{(\pm)}$ $(C_{(\pm)}{}^0)$	concentrations of ions in the reservoirs	m^{-3}
$\overline{C}_{(\pm)}(\overline{C}_{(\pm)}^0)$	concentrations of ions in the shale	m^{-3}
D_{eff}^f	effective (electro) diffusivity of the salt in the brine	$m^2\ s^{-1}$
$D_{(\pm)}{}^f$	self-diffusion coefficients of the ions in the brine	$m^2\ s^{-1}$
$M_{(\pm)}$	molecular weight of the ions	kg
$t_{(\pm)}$	microscopic Hittorf numbers of the ions	dimensionless
σ_f (σ_f^0)	conductivity of the solution in the reservoirs	$S\ m^{-1}$
$\overline{\sigma}_f(\overline{\sigma}f^0)$	conductivity of the pore fluid in the shale	$S\ m^{-1}$
Q_f	heat of transport of the pore fluid	$J\ m^{-3}$
ε_f	dielectric constant of the pore water	$F\ m^{-1}$
λ_f	thermal conductivity of the pore fluid	$J\ m^{-1}\ s^{-1}\ K^{-1}$
ρ_f	bulk density of the pore fluid	$kg\ m^{-3}$
$C_v{}^f$	specific heat per unit mass of the pore fluid	$J\ kg^{-1}\ °C^{-1}$
η_f	dynamic viscosity of the pore fluid	Pa s
$\mathbf{v}_f$	local velocity of the pore water	$m\ s^{-1}$
$\beta_{(\pm)}$	electromigration mobilities of the ions	$m^2\ s^{-1}\ V^{-1}$
$Q_{(\pm)}$	partial molar heats of transport of the ions	$J\ mol^{-1}$
$\Omega_{(\pm)}$	molecular volumes of cations and anions	m^3
Ω_w	molecular volume of the water molecules	m^3

Table 2. Material Properties of the Porous Shale

Property	Meaning	Unit
C_v	specific heat per unit mass of the porous shale	$J\ kg^{-1}\ K^{-1}$
CEC	cation exchange capacity	$C\ kg^{-1}$
D_{eff} (D_{eff}^0)	(electro) diffusivity of the salt in the shale	$m^2\ s^{-1}$
F	intrinsic electrical formation factor	dimensionless
f	intrinsic thermal formation factor	dimensionless
k	intrinsic permeability of the shale	m^2
q	charge per unit mass of the saturated shale	$C\ kg^{-1}$
$Q_V(Q_V^0)$	total charge per unit pore volume of the shale	$C\ m^{-3}$
$\overline{Q}_V(\overline{Q}_V^0)$	effective charge per unit pore volume of the shale	$C\ m^{-3}$
R	electrical conductivity dimensionless number	dimensionless
$T_{(\pm)}$ $(T_{(\pm)}^0)$	macroscopic Hittorf numbers	dimensionless
ε	brine filtration efficiency of the shale	dimensionless
γ	diffusivity efficiency of the porous shale	dimensionless
λ	intrinsic thermal conductivity of the shale	$J\ m^{-1}\ s^{-1}\ K^{-1}$
λ_g	thermal conductivity of the grains	$J\ m^{-1}\ s^{-1}\ K^{-1}$
$\sigma(\sigma_0)$	electrical conductivity of the shale	$S\ m^{-1}$
$\sigma_{(\pm)}$ $(\sigma_{(\pm)}^0)$	ionic contributions to the electrical conductivity	$S\ m^{-1}$
$L(L_0)$	electrokinetic coupling term	$A\ Pa^{-1}\ m^{-1}$
ρ_g	bulk density of the grains	$kg\ m^{-3}$
ϕ	connected porosity	dimensionless
Λ	characteristic length scale of the pore space	m
Θ	thermal conductivity dimensionless number	dimensionless

[6] 1. At the local scale, the ionic concentrations in the pore water are assumed to obey the Donnan distributions, an alternative to the Poisson-Boltzmann distributions in the equilibrium (thermostatic) state [e.g., *Lai et al.*, 1991; *Gu et al.*, 1997]. This allows to refer to average concentrations, osmotic pressure, and electrical potential in the pore space while Poisson-Boltzmann distributions implies that these quantities vary strongly with the distance to the pore water mineral interface.

[7] 2. We only consider linear disturbances in the vicinity of the thermostatic (equilibrium) state.

[8] 3. The pore water is assumed to be an ideal solution. This is appropriate for dilute solution only (<0.1 mol L^{-1}).

[9] 4. The porous medium is assumed to be isotropic and homogeneous at the scale of the representative elementary volume (however, we will briefly discussed anisotropy).

[10] 5. We assume local thermal equilibrium between the grains and the pore water.

[11] 6. For the sake of simplicity, we assume that the porous medium is rigid. However, the present theory could be generalized to the case of deformable porous materials by accounting for the Jacobian of the deformation tensor in the Lagrangian form of the constitutive equations.

[12] Chemical reactions and multiphase flow modeling are also kept for future investigations. Most of the parameters introduced in this paper are defined in Tables 1–3. The subscript and superscript zero describes the parameters in their thermostatic state.

2. Equilibrium State

[13] The system consists of two infinite brine reservoirs (hereinafter referred to as reservoirs I and II) separated by a water-saturated shale layer. The degree of compaction of the shale is high enough so that the macropores are not interconnected (Figure 1). We assume that the brine is dilute enough so that the thickness of the diffuse layer is comparable to the size of the micropores (Figure 1). For the sake of simplicity, the two reservoirs contain a single binary monovalent (1:1) salt (like NaCl or KCl) fully dissolved in water (the solvent). The (thermostatic) situation is characterized by the absence of any thermodynamic fluxes. In this equilibrium situation, we examine the concentrations of salt ions in the connected pore space of a representative elementary volume (REV) of a shale layer.

2.1. Excess Charge of Shales

[14] The matrix of shales is composed essentially of clay minerals and possibly some fine grains, which can play an important role (for example, carbonate grains would act as a buffer and control the pH of the pore water). Clay

Table 3. Fluxes and Thermodynamic Potentials

Property	Meaning	Unit
$\mathbf{H}$	macroscopic heat flux	$J\ m^{-2}\ s^{-1}$
$\mathbf{h}$	local heat flux	$J\ m^{-2}\ s^{-1}$
$\mathbf{J}_{(\pm)}$	macroscopic ionic fluxes	$mol\ m^{-2}\ s^{-1}$
$\mathbf{j}_{(\pm)}$	local ionic fluxes	$mol\ m^{-2}\ s^{-1}$
$\overline{\mathbf{J}}_{(\pm)}$	macroscopic ionic fluxes in the connected porosity	$mol\ m^{-2}\ s^{-1}$
$\mathbf{J}$	macroscopic current density	$A\ m^{-2}$
$\overline{\mathbf{J}}$	current density in the connected porosity	$A\ m^{-2}$
$\mathbf{U}$	Darcy or filtration velocity	$m\ s^{-1}$
$\tilde{\mu}_{(\pm)}(\tilde{\mu}_{(\pm)}^0)$	gravielectrochemical potentials of the ions	J
$\overline{\mu}_{(\pm)}(\overline{\mu}_{(\pm)}^0)$	local effective potentials of the ions	J
ψ	electrical potential (macroscopic disturbances)	V
φ (φ_0)	electrical double layer microscopic potential	V
p (p_0)	intrinsic fluid pressure in the pore space	Pa
$\overline{p}$	effective fluid pressure in the pore space	Pa
π (π_0)	osmotic pressure	Pa
T (T_0)	temperature	K

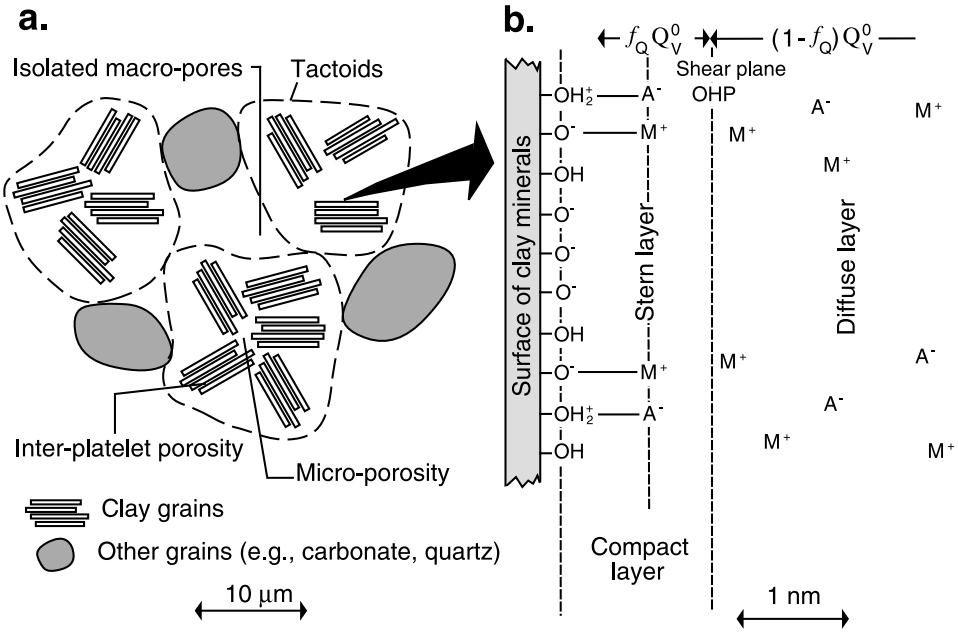

Figure 1. (a) Sketch of a silty shale. The porous composite comprises the pore space, the clay particles, and the other mineral grains. The pore space comprises the macroporosity, the microporosity, and the interlayer porosity for 2:1 clays like smectite. We assume that the macropores are isolated. In addition, we assume that the Gouy-Chapman diffuse layer extends over the entire microporosity. (b) Sketch of the electrical double-layer model. M represents the metal cations (e.g., Na^+ or K^+) and A represents the anions (e.g., Cl^-). The double layer comprises the Stern layer of sorbed counterions and the Gouy-Chapman diffuse layer. The total charge of the Stern and diffuse layers compensates the net charge of the mineral surface plus the net charge of the mineral framework associated with isormorphic substitutions in the mineral lattice.

minerals are usually negatively charged due to isomorphic substitutions inside the crystalline framework as well as chemical speciation between the surface reactive sites and the ions from the pore water [e.g., *Revil and Leroy*, 2001; *Leroy and Revil*, 2004]. An excess of charge of opposite sign counterbalances the charge deficiency of the clay minerals. This excess of charge is formed by a majority of counterions (e.g., Na^+) and a minor amount of "coions" (e.g., Cl^-). The cation exchange capacity, CEC (usually expressed in meq g^{-1}, where 1 meq g^{-1} = 96 320 C kg^{-1} in SI units [e.g., *Patchett*, 1975]) represents the excess of surface charge per unit weight of the minerals [e.g., *Ma and Eggleton*, 1999]. It is proportional to the specific surface area of the clay aggregate (surface area per unit weight) (Figure 2) and can be estimated from potentiometric adsorption measurements usually performed at pH 7. The CEC of the main clay minerals are given in Figure 2. For mixed layer clays, the CEC is a linear combination of the CEC of the end-members weighted by their relative proportions [*Gier*, 1998]. A more convenient way to express the CEC is to normalize the excess of charge per unit pore volume, which is noted Q_V (in C m^{-3}) [e.g., *Revil*, 1999]:

$$Q_V = \rho_g \left(\frac{1-\phi}{\phi} \right) \mathrm{CEC}, \tag{1}$$

where ρ_g represents the density of the grains and ϕ is the connected porosity. The charge density of the mineral grains (usually negative) is counterbalanced by a "countercharge" (generally positive) located in the pore network of the shale.

[15] There is however an additional complexity arising from the fact that the countercharge is partly located in the Stern layer directly at the surface of the minerals and partly in the diffuse (Gouy-Chapman) layer (Figure 1). We note f_Q the fraction of charge located in the Stern layer and $\overline{Q}_V \equiv (1 - f_Q)Q_V$ the net excess of charge per unit pore volume in the shale excluding the Stern layer ($f_Q Q_V$ represents the part of the countercharge located in the Stern layer, $(1 - f_Q)Q_V$ represents the fraction of the countercharge located in the Gouy-Chapman layer). We note $\overline{Q}_V{}^0$ the value taken by $\overline{Q}_V$ in the thermostatic state. The overall electroneutrality condition of the shale writes $\rho q = 0$, where

$$\rho q \equiv \frac{1}{V} \left(\int_{V_p} \overline{Q}_V^0 dV_p + \int_{S_w} Q_S dS + \int_{S_w} Q_0 dS \right), \tag{2}$$

where ρ is the bulk density of the shale and q is the charge per unit mass (so ρq represents the charge density of the shale), dV_p is an integration over the connected pore space, dS denotes an integration over the grain/pore water interface, Q_S represents the surface charge density in the Stern layer, and Q_0 represents the grain surface charge density (including a contribution associated with substitu-

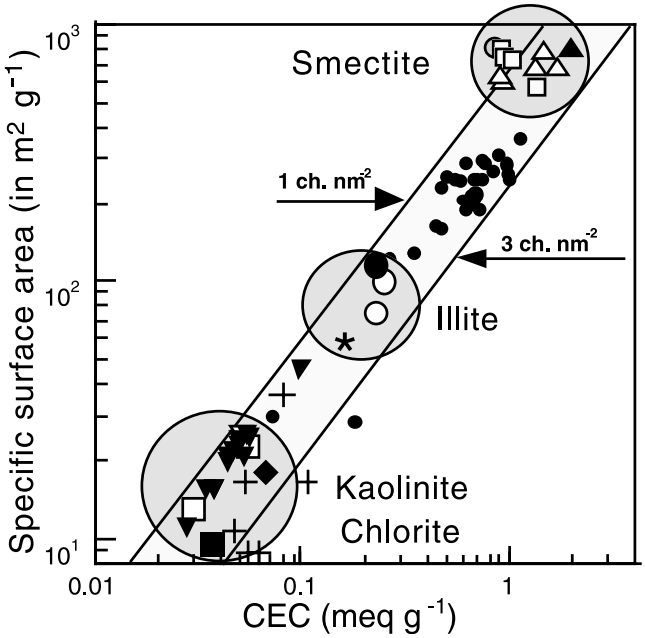

Figure 2. Specific surface area of clay minerals (in $m^2\,g^{-1}$) versus the CEC (in meq g^{-1} with 1 meq g^{-1} = 96,320 C kg^{-1} in SI units) for various clay minerals. The ratio between the CEC and the specific surface area gives the equivalent total surface charge density of the mineral surface. Experimental data are from 1, *Patchett* [1975] (small solid circles, shales with >50 clays; open triangles, montmorillonite; large open circles, illite; open squares, kaolinite); 2, *Lipsicas* [1984] (solid triangles, Vermiculite); 3, *Zundel and Siffert* [1985] (large solid circles, illite; large solid squares, kaolinite; solid losange, chlorite); 4, *Lockhart* [1980] (inverted open triangles, kaolinite); 5, *Sinitsyn et al.* [2000] (stars, illite); 6, *Avena and De Pauli* [1998] (grey solid circles: smectite); 7, *Shainberg et al.* [1988] (small squares, smectite); 8, *Su et al.* [2000] (crosses, shaly sands); and 9, *Ma and Eggleton* [1999, Table 3] (inverted solid triangles, kaolinite). The grey areas represent the domains of variations for kaolinite and chlorite, illite, and smectite.

tion in the crystalline framework). The electroneutrality condition yields

$$e\phi\left(\overline{C}^0_{(+)} - \overline{C}^0_{(-)}\right) + \frac{e}{V}\int_{S_w}\left(\Gamma^0_{(+)} - \Gamma^0_{(-)}\right)dS + \rho_g(1-\phi)\mathrm{CEC} = 0, \tag{3}$$

where e represents the elementary charge (positive, 1.6×10^{-19} C), $\Gamma^0_{(\pm)}$ is the surface density of counterions and coions (number of counterions per unit surface area) in the Stern layer, $\overline{C}^0_{(\pm)}$ represents the concentrations of counterions and coions in the pore space of the shale [*Leroy and Revil*, 2004]. The partition coefficient f_Q can be computed, in principle, from a TLM model and an iteration procedure from the following relationship:

$$f_Q = \frac{\int_{S_w}\left(\Gamma^0_{(+)} - \Gamma^0_{(-)}\right)dS}{V_p\left(\overline{C}^0_{(+)} - \overline{C}^0_{(-)}\right) + \int_{S_w}\left(\Gamma^0_{(+)} - \Gamma^0_{(-)}\right)dS}. \tag{4}$$

Using the recent model by *Leroy and Revil* [2004], we obtain very high values for f_Q above 085. This means that most of the countercharge is located in the Stern layer. However, we point out that f_Q is difficult to constrain.

2.2. Low Salinity Limit

[16] The shale layer is in contact with two uncharged porous bodies containing a 1:1 brine (NaCl, for example) at salinity C_f^0 (Figure 3). The cations and anions of the brine penetrate the connected porosity of the shale until a thermodynamic equilibrium is reached. Note that the establishment of this equilibrium state is not instantaneous. The electrical field associated with charge deficiency of the clay minerals is shielded very efficiently by the countercharge. The macroscopic average of the local electrical field is zero, but there is a net electrical potential in the pore space of the shale.

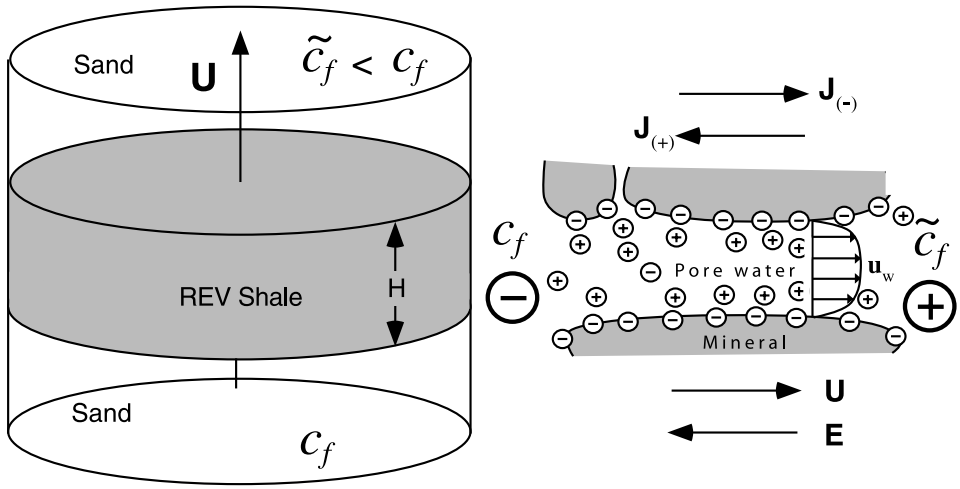

Figure 3. Sketch of the filtration of a 1:1 salt through a shale. The direction of the Darcy velocity **U**, the electrokinetic component of the electrical field **E**, and the electrokinetically induced ionic density fluxes are shown on the right side. The salinity of the effluent is noted $\tilde{C}_f$, while the salinity of the pore water forced into the shale is noted C_f.

[17] In the uncharged porous bodies the chemical potentials of the ions and water (i.e., the solvent) are defined by

$$\mu^0_{(\pm)} = \mu^R_{(\pm)} + k_b T_0 \ln C^0_{(\pm)} \tag{5}$$

$$\mu^0_w = \mu^R_w + \Omega_w p_0 + k_b T_0 \ln C^0_w, \tag{6}$$

where k_b is the Boltzmann constant (1.381×10^{-23} J K^{-1}), T_0 is the temperature (in K), and $\mu_{(+)}$, $\mu_{(-)}$, μ_w represent the chemical potentials of cations, anions, and water respectively, $C_{(+)}$, $C_{(-)}$, C_w are the volumetric concentrations of cations, anions, and water, respectively, Ω_w is the molecular volume of water, p is the pressure of water ($p_0 = \rho_f g z$ is the pressure due to the gravity body force), and the superscript and subscript 0 and R in equations (5) and (6) refer to the thermostatic state and a distinct reference state, respectively. The reference state corresponds to unit molar concentrations of the ionic species and to the isoelectric point for the shale, i.e., conditions for which the effective surface electrical potential of the clays is equal to zero (i.e., $Q_0 = 0$, the shale becomes an uncharged material).

[18] In the shale, the electrochemical potentials of the ions and water are given by

$$\overline{\mu}^0_{(\pm)} = \overline{\mu}^R_{(\pm)} + k_b T_0 \ln \overline{C}^0_{(\pm)} \pm e\overline{\varphi}_0 \tag{7}$$

$$\overline{\mu}^0_w = \overline{\mu}^R_w + \Omega_w \overline{p}_0 + k_b T_0 \ln \overline{C}^0_w, \tag{8}$$

where $\overline{\varphi}_0$ and $\overline{p}_0$ are the electrical potential and pore fluid pressure in the pore water of the shale (in the thermostatic state). The overbar refers to the pore water of the shale, and the superscript 0 and R indicate that the concerned quantities are taken in the thermostatic and reference states, respectively. Note that electrical potential and pore fluid pressure refer to a single electrical potential and fluid pressure rather than a spatial distribution of these.

[19] Thermodynamic equilibrium between the brine in the reservoirs and the pore water of the shale takes the form of an equality between the chemical potential of the pore water of the shale and that of the brine in both the thermostatic and reference states,

$$\mu^0_{(\pm)} = \overline{\mu}^0_{(\pm)}, \tag{9}$$

$$\mu^R_{(\pm)} = \overline{\mu}^R_{(\pm)}, \tag{10}$$

$$\mu^0_w = \overline{\mu}^0_w, \tag{11}$$

$$\mu^R_w = \overline{\mu}^R_w. \tag{12}$$

Conservations of charge and mass in the pore water of the shale and in the brine reservoir are

$$\overline{C}^0_{(+)} = \overline{C}^0_{(-)} + \overline{Q}^0_V/e, \tag{13}$$

$$C^0_{(-)} = C^0_{(+)} = C^0_f, \tag{14}$$

$$\Omega_w \overline{C}^0_w + \Omega_{(+)} \overline{C}^0_{(+)} + \Omega_{(-)} \overline{C}^0_{(-)} = 1, \tag{15}$$

$$\Omega_w C^0_w + \left(\Omega_{(+)} + \Omega_{(-)}\right) C^0_f = 1, \tag{16}$$

where C^0_f is the salinity of the brine in the reservoirs, and $\Omega_{(\pm)}$ are the molecular volumes of cations and anions. Equation (13) is a consequence of equations (3) and (4). After some algebraic manipulations, equations (5), (7), (9), and (10) yield a modified version of the Donnan equilibrium conditions accounting for the partition of the counterions between the Stern and Gouy-Chapman layers:

$$C^0_{(+)} C^0_{(-)} = \overline{C}^0_{(+)} \overline{C}^0_{(-)}, \tag{17}$$

$$\overline{C}^0_{(\pm)} = C^0_f \exp\left(-\frac{(\pm e)\overline{\varphi}_0}{k_b T_0}\right), \tag{18}$$

$$\overline{\varphi}_0 = -\frac{k_b T_0}{2e} \ln\left(\frac{\overline{C}^0_{(+)}}{\overline{C}^0_{(-)}}\right). \tag{19}$$

Combining equations (13) and (17) yields a second-order equation:

$$\overline{C}^{0\,2}_{(+)} - \left(\overline{Q}^0_V/e\right)\overline{C}^0_{(+)} - C^0_{(+)} C^0_{(-)} = 0. \tag{20}$$

The solution of (20) combined with (18) yields

$$\overline{C}^{0\,2}_{(\pm)} = \left(\frac{\overline{Q}^{0\,2}_V}{4e^2} + C^{0\,2}_f\right)^{1/2} \pm \frac{\overline{Q}^0_V}{2e}, \tag{21}$$

$$\overline{\varphi}_0 = -\frac{k_b T_0}{2e} \ln\left[\frac{\sqrt{\overline{Q}^{0\,2}_V + 4e^2 C^{0\,2}_f} + \overline{Q}^0_V}{\sqrt{\overline{Q}^{0\,2}_V + 4e^2 C^{0\,2}_f} - \overline{Q}^0_V}\right]. \tag{22}$$

Equations (21) and (22) characterize the thermostatic state. Equation (21) corresponds to a modified version of the Teorell-Meyer-Siever (TMS) model [*Teorell*, 1935; *Meyer and Sievers*, 1936]. It provides the mean ionic concentrations inside the charged material, in the equilibrium state, as a function of the concentrations of the ionic species contained in the brine reservoir. Let us consider for example kaolinite with $\phi = 0.30$ (30% porosity), CEC = 0.04 meq g^{-1} (Figure 2), in contact with a reservoir containing a sodium chloride solution at 10^{-3} mol L^{-1}. The grain mass

density is expected to be higher than the measured value reported in the literature (typically ρ_g = 2580 kg m^{-3}), which includes the two hydration layers of the clay mineral. Taking into consideration the unit cell parameters of a perfect kaolinite hexagonal crystal ($Al_4[Si_4O_{10}](OH)_8$): a = 0.5139 nm, b = 0.8932 nm, c = 0.7371 nm, $\alpha = \gamma = 90°$, and $\beta = 104.8°$, the volume of this elementary cell is ($a\ b\ c \sin\beta$) = 0.3271 nm^3, its molecular weight 516.4 g mol^{-1}, and therefore its density is equal to ρ_g = 2620 kg m^{-3}. With this grain density, this yields $Q_V^0 = 2.38 \times 10^7$ C m^{-3}. Taking f_Q = 0.90, this corresponds to 2.47×10^{-2} mol L^{-1} equivalent charge. Use of equation (21) yields $\overline{C}^0_{(+)} = 2.474 \times 10^{-2}$ mol L^{-1} and $\overline{C}^0_{(-)} = 4.04 \times 10^{-5}$ mol L^{-1} for the concentrations of counterions and coions, respectively. So the amount of coions contained in the pore water of the shale is extremely small by comparison with the number of counterions. Such a state is characteristic of clay-rich materials.

[20] The osmotic pressure is given by the Van't Hoff relationship

$$\pi_0 \equiv \overline{p}_0 - p_0 = -\frac{k_b T_0}{\Omega_w} \ln\left(\frac{\overline{C}^0_w}{C^0_w}\right), \tag{23}$$

$$\pi_0 \approx k_b T_0 \left(\overline{C}^0_{(+)} + \overline{C}^0_{(-)} - 2C^0_f\right), \tag{24}$$

$$\pi_0 \approx 2k_b T_0 C^0_f \left[\cosh\left(\frac{e\overline{\varphi}_0}{k_b T_0}\right) - 1\right], \tag{25}$$

where we have neglected the difference between the molecular volume of the water and that of the ions. For very dilute pore water, the osmotic pressure is given by $\pi_0 \approx k_b T_0 \overline{Q}^0_V / e$. Taking, for example, $\overline{Q}^0_V = 2.38 \times 10^6$ C m^{-3}, $k_b = 1.381 \times 10^{-23}$ J K^{-1}, and T_0 = 298 K yields $\pi_0 \approx$ 61 kPa. A possible value of $\overline{Q}^0_V = 23.8 \times 10^6$ C m^{-3} yields $\pi_0 \approx$ 0.61 MPa. So the osmotic pressure can reach very high values in shales. For smectites the osmotic pressure can be higher than 5 MPa. Note that there is another osmotic pressure contribution due to hydration forces between surfaces [*Besseling*, 1997]. However, the strength of the hydration force decreases rapidly with the distance between adjacent surfaces and affects only the interlayer porosity of 2:1 clays like smectites.

2.3. High Salinity Limit

[21] In the high salinity limit (typically >0.5 mol L^{-1}) the diffuse layer disappears and the counterions are packed in the Stern layer. Outside the Stern layer the pore water has the same salinity as the pore water in the reservoir in contact with the shale layer. In this situation, which is not analyzed in this paper [see *Revil*, 1999] we expect the transport properties to be rather different than in the dilute limit considered here.

3. Volume-Averaging Approach and Local Equations

[22] We specify now the local equations in the vicinity of the thermostatic equilibrium state. We also describe the volume averaging approach used in the following sections.

3.1. Volume-Averaging Approach

[23] We consider the shale to be a random porous medium of volume V composed of the connected pore region of volume V_p and the grains of volume V_g ($V = V_p + V_g$). We note S_w the surface area between the grain and the connected pore space. The characteristic functions of the pore region θ and pore-solid interface M are defined by

$$\theta(\mathbf{r}) = \begin{cases} 1, \mathbf{r} \in V_p, \\ 0, \mathbf{r} \in V_g, \end{cases} \tag{26}$$

$$M(\mathbf{r}) = |\nabla\theta(\mathbf{r})|, \tag{27}$$

respectively. The volume average of a vector **a** (or a scalar) is defined by

$$\langle \mathbf{a} \rangle \equiv \mathbf{A} \equiv \frac{1}{V} \int_V \{\theta(\mathbf{r})\mathbf{a} + [1 - \theta(\mathbf{r})]\mathbf{a}\} dV, \tag{28}$$

$$\langle \mathbf{a} \rangle \equiv \mathbf{A} \equiv \frac{1}{V} \left[\int_{V_p} \mathbf{a} dV_p + \int_{V_g} \mathbf{a} dV_g\right]. \tag{29}$$

The pore water phase average is defined by

$$\overline{\mathbf{A}} \equiv \frac{1}{V_p} \int_{V_p} \mathbf{a} dV_p. \tag{30}$$

[24] The porosity and specific surface area are defined as the volume average of the function $\theta(\mathbf{r})$ and $M(\mathbf{r})$, respectively, i.e.,

$$\phi \equiv \langle \theta(\mathbf{r}) \rangle, \tag{31}$$

$$\alpha \equiv S/V = \langle M(\mathbf{r}) \rangle, \tag{32}$$

where α is the average interfacial area per unit total volume. Although we assume isotropy in this paper, a few words on extension to anisotropic situations is needed since this model involves shales, which are usually anisotropic. *Bercovici et al.* [2001] define a fabric tensor as

$$\boldsymbol{\alpha} \equiv \frac{1}{V} \int_V \frac{\nabla\theta(\mathbf{r}) \nabla\theta(\mathbf{r})}{|\nabla\theta(\mathbf{r})|} dV, \tag{33}$$

which is symmetric by construction. The trace of this tensor is $\mathrm{Tr}(\boldsymbol{\alpha}) = \alpha$ and if the system is isotropic $\boldsymbol{\alpha} = (\alpha/3)\mathbf{I}$, where $\mathbf{I}$ is the identity matrix. In anisotropic media, transport properties like permeability, electrical conductivity, and thermal conductivity are related to the fabric tensor $\boldsymbol{\alpha}$. However, the isotropic model developed hereafter is already complex enough (10 independent material properties to

determine) to keep a rigorous anisotropic theory for future investigations.

[25] Slattery's theorem yields [e.g., *Slaterry*, 1981; *Howes and Whitaker*, 1985]

$$\langle \nabla a \rangle = \nabla \langle a \rangle + \frac{1}{V} \int_{S_w} a \mathbf{n} dS \tag{34}$$

$$\langle \nabla \cdot \mathbf{a} \rangle = \nabla \cdot \mathbf{A} + \frac{1}{V} \int_{S_w} \mathbf{n} \cdot \mathbf{a} dS, \tag{35}$$

where $\mathbf{n}$ is the unit vector normal to the pore-solid interface and directed from the pore solution to the solid when $\mathbf{a}$ is defined in the connected pore space and from the solid to the pore solution when $\mathbf{a}$ is defined in the matrix.

[26] Each state variable characterizing the system is considered as the sum of a term corresponding to the thermostatic state and a perturbation. For example, the concentrations, the electrical field, the electrical potential, and the temperature in the bulk pore water are written as

$$\overline{C}_{(\pm)} = \overline{C}^0_{(\pm)} + \overline{c}_{(\pm)}, \tag{36}$$

$$\mathbf{E} = \mathbf{E}^0_f + \mathbf{e}_f, \tag{37}$$

$$\overline{\varphi} = \overline{\varphi}_0 + \delta\overline{\varphi}, \tag{38}$$

$$T = T_0 + \delta T, .. \tag{39}$$

where $\mathbf{E}_f^0 = -\nabla\ \overline{\varphi}_0$, $\mathbf{e}_f = -\nabla\delta\overline{\varphi} - \nabla\psi$($\psi$ is the local potential associated with the existence of a macroscopic electrical field at the scale of the system, see below) and so on. The first term represents the thermostatic state while the second term represents deviation from equilibrium. The determination of the variation $\delta\overline{\varphi} = \overline{\varphi} - \overline{\varphi}_0$ can be obtained from the TLM approach by solving the TLM equations in the new set of thermodynamic conditions [*Leroy and Revil*, 2004].

[27] The next step is to upscale the local equations. We consider that the driving forces are sufficiently weak so we can linearize the local equations and keep only first-order terms for which linear thermodynamics applies and Onsager's reciprocal relationships hold. As a consequence, all dispersive phenomena are ignored in the present model.

[28] To complete the averaging procedure, we define the representative elementary volume as an averaging disk of porous shale delimited by two large plane-parallel circular faces of area A separated by distance H ($V = A\,H$) (Figure 3). The disk is comprised between the two reservoirs defined in section 2. A potential difference can be defined between the two reservoirs. By dividing each potential difference by H, one obtains the appropriate macroscopic field in the direction normal to the disk faces (e.g., temperature gradient, pressure gradient, electrical field). The normal to the disk faces is defined as the z direction of unit vector $\hat{\mathbf{z}}$ such that we have

$$\hat{\mathbf{z}} \cdot \mathbf{E} = -\frac{\Delta\psi}{H}, \tag{40}$$

$$\Delta\psi \equiv \psi(H) - \psi(0), \tag{41}$$

for the macroscopic electrical field, for example. Similar macroscopic boundary conditions can be defined for the ionic concentrations, the pore fluid pressure, and the temperature.

[29] The final purpose of the volume-averaging approach is to show that the constitutive relationships for the fluxes obey linear relationships with respect to the thermodynamic forces:

$$\begin{bmatrix} \mathbf{J}_{(+)} \\ \mathbf{J}_{(-)} \\ \mathbf{U} \\ \mathbf{H} \end{bmatrix} = -\mathbf{L} \begin{bmatrix} \nabla\tilde{\mu}_{(+)} \\ \nabla\tilde{\mu}_{(-)} \\ \nabla\overline{p} \\ \nabla T/T_0 \end{bmatrix}, \tag{42}$$

where $\mathbf{L}$ is a 4×4 matrix with components L_{ij}, $\mathbf{J}_{(\pm)}$ are the macroscopic ionic fluxes, $\mathbf{U}$ is the filtration (Darcy) velocity (in m s^{-1}), $\mathbf{H}$ is the heat flux, $\tilde{\mu}_{(\pm)}$ is the gravielectrochemical potentials, and $\overline{p}$ is the effective fluid pressure including osmotic and gravitational contributions.

3.2. Local Equations in the Connected Porosity

[30] In a Newtonian fluid the local ionic densities $\mathbf{j}_{(\pm)}$ and heat flux $\mathbf{h}$ are related to the gradient of the electrochemical potentials $\nabla\tilde{\mu}_{(\pm)}$ and to the gradient of the temperature ∇T by the generalized Nernst-Planck equations [*Nernst*, 1888; *Planck*, 1890; *De Groot and Mazur*, 1984, Chapter XI]

$$\begin{bmatrix} \mathbf{j}_{(+)} - \overline{C}_{(+)}\mathbf{v}_f \\ \mathbf{j}_{(-)} - \overline{C}_{(-)}\mathbf{v}_f \\ \mathbf{h} - Q_f\mathbf{v}_f \end{bmatrix} = -\begin{bmatrix} \frac{\beta_{(+)}\overline{C}_{(+)}}{e} & 0 & \frac{\beta_{(+)}\overline{C}_{(+)}Q_{(+)}}{e} \\ 0 & \frac{\beta_{(-)}\overline{C}_{(-)}}{e} & \frac{\beta_{(-)}\overline{C}_{(-)}Q_{(-)}}{e} \\ \frac{\beta_{(+)}\overline{C}_{(+)}Q_{(+)}}{e} & \frac{\beta_{(-)}\overline{C}_{(-)}Q_{(-)}}{e} & \lambda_f T_0 \end{bmatrix} \cdot \begin{bmatrix} \nabla\tilde{\mu}_{(+)} \\ \nabla\tilde{\mu}_{(-)} \\ \nabla T/T_0 \end{bmatrix}, \tag{43}$$

where $\mathbf{v}_f$ is the local velocity of the pore water and the other properties are defined in Table 1. Some values of the mobilities $\beta_{(\pm)}$ and partial molar heats of transport $Q_{(\pm)}$ are given in Table 4. The heats of transport represent the heats transported along with a unit diffusion flux of anions and cations. The heat of transport $Q_f = \rho_f C_v^f T_0$ is defined as the heat flux that occurs during isothermal water flow [*Chu et al.*, 1983]. The gradients of the electrochemical potentials are

$$\nabla\tilde{\mu}_{(\pm)} = k_b T \nabla \ln \overline{C}_{(\pm)} - (\pm 1) e\mathbf{E}. \tag{44}$$

Note that for the ions the gravitational component can be ignored by comparison with the strength of the other contributions.

Table 4. Properties of Some Selected Ions at 25°C at Infinite Dilution

Ion	Na^+	K^+	Cl^-
$\beta_{(\pm)}$, $m^2\ s^{-1}\ V^{-1}$	5.19×10^{-8}	7.61×10^{-8}	8.47×10^{-8}
$Q_{(\pm)}$,[a] $J\ mol^{-1}$	3.46×10^{-3}	2.59×10^{-3}	0.53×10^{-3}

[a]From *Lin* [1991].

[31] The equation for the velocity of the pore fluid is the Navier-Stokes equation

$$\rho_f\left(\frac{\partial \mathbf{v}_f}{\partial t} + \mathbf{v}_f \cdot \nabla \mathbf{v}_f\right) = -\nabla p - \left(\frac{Q_f}{T_0}\right)\nabla T + \eta_f \nabla^2 \mathbf{v}_f + \mathbf{F}_w + \mathbf{F}_{(+)} + \mathbf{F}_{(-)}, \tag{45}$$

where t is time and $\mathbf{F}_i$ is the external (body) force per unit volume acting on the component i. Equation (45) is nothing else but a force balance equation for a representative elementary volume element of the pore fluid. We consider that the viscosity of the pore water is not altered by the existence of a net electrical field inside the pore network of the shale. Indeed, except for the two first hydration layers of the mineral surface, thermal motion in the pore water dominates electroviscous effects.

[32] The bulk forces applied to water are the gravity force, the electrical force (as the free charge density is unbalanced in the bulk pore water of the shale), and the thermal force. Indeed, a temperature gradient gives rise to an equivalent pressure gradient called the thermomolecular or thermo-osmotic pressure. This pressure is usually difficult to observe because it is easily obscured by thermomechanical and convective effects. The thermomolecular pressure is produced by an increase, in a temperature field, of the number of collisions between molecules. Each molecule receives a higher number of collisions from the direction where the temperature is the highest than from the opposite direction. This creates a global motion of the pore fluid, by viscous coupling, in the direction of the temperature field. This phenomenon has nothing to do with convection associated with buoyancy.

[33] The body forces that apply to the pore water and to the ions are

$$\mathbf{F}_w \approx \rho_f \mathbf{g} + Q_f \nabla T / T_0, \tag{46}$$

$$\mathbf{F}_{(\pm)} = \rho_{(\pm)}\mathbf{g} \pm e\overline{C}_{(\pm)}\mathbf{E} \approx \pm e\overline{C}_{(\pm)}\mathbf{E}. \tag{47}$$

In the assumption of slow incompressible viscous flow with a vanishingly small Reynolds number (Stokes fluid), the local fluid velocity is a solution of the Stokes problem described by the Stokes equation plus the continuity (mass balance) equation

$$-\nabla p + \eta_f \nabla^2 \mathbf{v}_f + \mathbf{F}_f = 0, \tag{48}$$

$$\nabla \cdot \mathbf{v}_f = 0, \tag{49}$$

$$\mathbf{F}_f = \mathbf{F}_w + \mathbf{F}_{(+)} + \mathbf{F}_{(-)} = \rho_f \mathbf{g} + \overline{Q}_V \mathbf{E} + Q_f \nabla T / T_0, \tag{50}$$

and $\mathbf{v}_f = 0$ on S_W. In equation (50), $\overline{Q}_V = (1 - f_Q)Q_V = e(\overline{C}_{(+)} - \overline{C}_{(-)})$ represents the excess of charge per unit volume in the pore space of the shale in the thermodynamic state (section 2.1). Using the Hodge decomposition for an arbitrary vector F arising in the Stokes problem, *Avellaneda and Torquato* [1991] showed that the hydrodynamical response of the Stokes fluid is identical to the response obtained if F is replaced by $\upsilon\mathbf{E}$, where υ is a constant and $\mathbf{E}$ is the electrical field. This means that the expected hydrodynamic response for a temperature field will be similar to that given by the application of an electrical field. The reason for this is that, for steady state conditions, the gradient of the scalar potential in the Hodge decomposition of F corresponds to a fluctuation of the pore pressure that does not affect the pore fluid velocity field.

[34] We summarize now the key equations of the electrodynamic problem. The electrical field is a solution of the local Poisson problem

$$\varepsilon_f \nabla \cdot \mathbf{E} = \overline{Q}_V \tag{51}$$

$$\mathbf{E} = -\nabla \overline{\psi}, \tag{52}$$

where ε_f is the dielectric constant of the pore water. The combination of the local Stokes and Poisson problems yields

$$\nabla \cdot \overline{\overline{\sigma}}_f + \rho_f \mathbf{g} = 0, \tag{53}$$

$$\overline{\overline{\sigma}}_f = -p\overline{\overline{I}} + \overline{\overline{\sigma}}_f^V + \overline{\overline{T}}_f^M - \rho_f C_\upsilon^f T \overline{\overline{I}}, \tag{54}$$

$$\overline{\overline{T}}_f^M = \varepsilon_f\left(\mathbf{E} \otimes \mathbf{E} - \mathbf{E}^2\overline{\overline{I}}/2\right), \tag{55}$$

where $\overline{\overline{\sigma}}_f$ is the Cauchy stress tensor of the pore fluid, $\overline{\overline{\sigma}}_f^V$ and $\overline{\overline{T}}_f^M$ (positive in tension) represent the viscous contribution to the Cauchy stress tensor and the Maxwell stress tensor in the pore fluid, respectively (with the property $\nabla \cdot \overline{\overline{T}}_f^M = \overline{Q}_V\mathbf{E}$), and $\mathbf{E} \otimes \mathbf{E}$ represents a dyadic product between vectors.

3.3. Effective Electrical Potential and Fluid Pressure

[35] The electrical potential in the pore space is the sum of two contributions. The first is due to the electrical double layer and the second results from the existence of macroscopic thermodynamic disequilibrium conditions resulting in ions migration. This yields $\overline{\psi} = \overline{\varphi} + \psi$, where $\overline{\varphi}$ results from (microscopic) electrical double layer effects, whereas ψ results from macroscopic disturbances affecting the migration of the ionic species. So the electrical body force $(\mathbf{F}_{(+)} + \mathbf{F}_{(-)})$ entering the Stokes equation is split into two contributions

$$\mathbf{F}_{(+)} + \mathbf{F}_{(-)} = -\overline{Q}_V \nabla \overline{\psi}, \tag{56}$$

$$\mathbf{F}_{(+)} + \mathbf{F}_{(-)} = -\overline{Q}_V \nabla \overline{\varphi} - \overline{Q}_V \nabla \psi. \tag{57}$$

The first contribution is responsible for swelling pressure whereas the second contribution is responsible for various

electro-osmotic contributions in the Stokes equation. Equating the chemical potentials of the ions present in the pore space with that of a fictitious salt solution locally in equilibrium with the local pore water solutions yields [e.g., *Moyne and Murad*, 2002]

$$\overline{C}_{(\pm)} = C_f \exp\left[-\frac{(\pm e)\overline{\varphi}}{k_b T}\right] \tag{58}$$

$$\overline{Q}_V = e\left(\overline{C}_{(+)} - \overline{C}_{(+)}\right) = -2eC_f \sinh\left[\frac{e\overline{\varphi}}{k_b T}\right], \tag{59}$$

which extends equation (18) to the thermodynamic state. Incorporating $-\overline{Q}_V \nabla \overline{\varphi}$ and the body force due to gravity into the pore fluid pressure gradient term define an effective pore fluid pressure as

$$\overline{p} = p + \int_0^{\overline{\varphi}} \overline{Q}_V d\overline{\varphi}' + \rho_f g z, \tag{60}$$

$$\overline{p} = p - 2eC_f \int_0^{\overline{\varphi}} \sinh\left[\frac{e\overline{\varphi}'}{k_b T}\right] d\overline{\varphi}' + \rho_f g z, \tag{61}$$

$$\overline{p} = p - 2C_f k_b T\left[\cosh\left(\frac{e\overline{\varphi}}{k_b T}\right) - 1\right] + \rho_f g z, \tag{62}$$

$$\overline{p} = p - k_b T\left[\overline{C}_{(+)} + \overline{C}_{(-)} - 2C_f\right] + \rho_f g z, \tag{63}$$

$$\overline{p} = p - \pi + \rho_f g z, \tag{64}$$

(z positive upward by convention) and $\nabla \overline{p} = \nabla (p - \pi) - \rho_f \mathbf{g}$. The swelling pressure is given by the Van't Hoff relationship, as in the thermostatic case

$$\pi = k_b T\left(\overline{C}_{(+)} + \overline{C}_{(-)} - 2C_f\right), \tag{65}$$

and in the dilute case, $\pi \approx k_b T \overline{Q} V/e$. Note that the osmotic pressure is a natural consequence of the overlapping between the diffuse layers of adjacent mineral surfaces in the microporosity. Similar to the electrical potential, the pore fluid effective pressure is the sum of the pore fluid pressure of a fictitious solution in local equilibrium with the pore water and a swelling pressure term due to electrical double layer interaction effects. The motivation for the introduction of the effective fluid pressure lies in the fact that gradients in both hydrostatic and osmotic pressure can produce flow of the pore fluid. The Stokes problem becomes

$$-\nabla \overline{p} + \eta_f \nabla^2 \mathbf{v}_f + \rho_f C_v^f \nabla T - \overline{Q}_V \nabla \psi = 0 \tag{66}$$

$$\nabla \cdot \mathbf{v}_f = 0. \tag{67}$$

4. Conductivity Terms

[36] We first specify here a set of relationships between the texture that we wish to characterize by a minimum set of textural parameters, and the four macroscopic conductivity terms entering the macroscopic constitutive equation (42).

4.1. Electrical Conductivity

[37] The conductivity terms L_{11} and L_{22} are obtained by upscaling the ionic fluxes in absence of all the driving forces except the electromotive force (i.e., the electrical potential difference applied on the two reservoirs). The pore water phase average of the macroscopic current density (see equation (30)) is

$$\overline{\mathbf{J}}_{(\pm)} = \frac{1}{V_p} \int_{V_p} \mathbf{j}_{(\pm)} dV_p, \tag{68}$$

$$\overline{\mathbf{J}}_{(\pm)} = \frac{-(\pm 1)\beta_{(\pm)}}{V_p} \int_{V_p} \overline{C}_{(\pm)} \mathbf{E} dV_p, \tag{69}$$

$$\overline{\mathbf{J}}_{(\pm)} = \frac{-(\pm 1)\beta_{(\pm)} \overline{C}^0_{(\pm)}}{V_p} \int_{V_p} \mathbf{e}_f dV_p, \tag{70}$$

$$\overline{\mathbf{J}}_{(\pm)} = \frac{(\pm 1)\beta_{(\pm)} \overline{C}^0_{(\pm)}}{V_p} \int_{V_p} \nabla \psi dV_p, \tag{71}$$

$$\overline{\mathbf{J}}_{(\pm)} = \frac{(\pm 1)\beta_{(\pm)} \overline{C}^0_{(\pm)} \Delta\psi}{V_p H} \int_{V_p} \nabla \Gamma dV_p, \tag{72}$$

where we have kept only first-order terms and where the Γ field satisfies the following boundary value fundamental problem [*Pride*, 1994]:

$$\nabla^2 \Gamma = 0, \mathbf{r} \in V_p, \tag{73}$$

$$\mathbf{n}.\nabla \Gamma = 0, \mathbf{r} \in S_w, \tag{74}$$

$$\Gamma = \begin{cases} H, & \text{on } z = H, \\ 0, & \text{on } z = 0. \end{cases} \tag{75}$$

Using Slaterry's theorem (equation (34)) yields

$$\overline{\mathbf{J}}_{(\pm)} = \frac{(\pm 1)\beta_{(\pm)} \overline{C}^0_{(\pm)} \Delta\psi}{\phi H} \left[\nabla\left(\frac{1}{V} \int_{V_p} \Gamma dV_p\right) + \frac{1}{V} \int_{S_w} \mathbf{n} \Gamma dS\right], \tag{76}$$

$$\overline{\mathbf{J}}_{(\pm)} = \frac{(\pm 1)\beta_{(\pm)} \overline{C}^0_{(\pm)}}{\phi} \left[\phi + \frac{\hat{\mathbf{z}}}{V}. \int_S \mathbf{n} \Gamma dS\right] \left(\frac{\Delta\psi}{H}\right) \hat{\mathbf{z}}, \tag{77}$$

$$\overline{\mathbf{J}}_{(\pm)} = -(\pm 1) \frac{\beta_{(\pm)} \overline{C}^0_{(\pm)}}{F\phi} \nabla \psi, \tag{78}$$

where F is the so-called electrical formation factor defined by

$$\frac{1}{F} = \phi + \frac{\hat{\mathbf{z}}}{V}.\int_S \mathbf{n}\Gamma dS. \quad (79)$$

The formation factor can be also determined by averaging the Joule dissipation of energy. This yields the representation formula $1/F = \langle \mathbf{e}.\mathbf{e} \rangle$where angle brackets represent the volume average (29) and $\mathbf{e} \equiv -\mathbf{E}/(\Delta\psi/H)$ is a normalized electrical field, i.e., the local electrical field divided by the modulus of the volume-averaged electrical field given by equations (40) and (41). In both case, the formation factor represents the fraction of the connected porosity that controls migration of the charge carriers through the connected pore space. The tortuosity α_∞ ($\geq$ 1) is defined by $\alpha_\infty \equiv F\phi$.

[38] The ionic contributions $\overline{\sigma}^0_{(\pm)}$ to the electrical conductivity $\overline{\sigma}_f{}^0$ of the pore fluid in the shale are defined by

$$\overline{\mathbf{J}}_{(\pm)} = -\frac{(\pm 1)\overline{\sigma}^0_{(\pm)}}{e\alpha_\infty}\nabla\psi, \quad (80)$$

$$\overline{\sigma}^0_{(\pm)} = \overline{C}^0_{(\pm)}\beta_{(\pm)}e. \quad (81)$$

The pore water phase average of the electrical current associated with the connected porosity is

$$\overline{\mathbf{J}} = e\left(\overline{\mathbf{J}}_{(+)} - \overline{\mathbf{J}}_{(-)}\right) = -\left(\overline{\sigma}^0_f/\alpha_\infty\right)\nabla\psi. \quad (82)$$

We introduce the key dimensionless number

$$R \equiv \frac{\overline{Q}^0_V}{2eC^0_f} = \frac{(1-f_Q)Q^0_V}{2eC^0_f}, \quad (83)$$

which represents the excess of counterions contained in the pore water of the shale divided by the brine concentration. In the low salinity domain we use the results obtained in section 2.3 using the Donnan equilibrium assumption. Taking equations (21), (78), (82), and (83) yields the electrical conductivity of the shale and its ionic contributions:

$$\overline{\sigma}^0_f = C^0_f e\left[\left(R + \sqrt{R^2+1}\right)\beta_{(+)} + \left(-R + \sqrt{R^2+1}\right)\beta_{(-)}\right] \quad (84)$$

$$\overline{\sigma}^0_{(\pm)} = C^0_f e\beta_{(\pm)}\left(\sqrt{R^2+1} + (\pm 1)R\right). \quad (85)$$

The electrical conductivity of the brine in the reservoir in contact with the shale is $\sigma^0_f = e(C^0_{(+)}\ \beta_{(+)} + C^0_{(-)}\ \beta_{(-)})$, where $\beta_{(\pm)}$ represents the mobility of cations or anions (Table 4) and $C^0_f = C^0_{(+)} = C^0_{(-)}$(salinity in the two reservoirs). If the mobility of cations and anions are similar, as is the case for NaCl and KCl solutions, the electrical conductivity of the pore water in the shale is given by $\overline{\sigma}_f{}^0 \approx \sigma_f{}^0\sqrt{1+R^2}$, i.e., the conductivity of the pore water of the shale is always higher than the electrical conductivity of the brine in the reservoir in contact with the shale. In addition, we observe that the electrical conductivity of the pore water in the shale is a nonlinear function of the dimensionless number R. The asymptotic behavior of these equations yields a low salinity limit $\overline{\sigma}_f{}^0$ ($R \gg 1$) = $\overline{Q}^0_V\ \beta_{(+)}$. Taking $\beta_{(+)}(Na^+$, 25°C) = 5.19 × 10^{-8} m^2 s^{-1} V^{-1} (Table 4) and $\overline{Q}^0_V$ = 2.38 × 10^6 C m^{-3} yields $\overline{\sigma}_f{}^0$(R ≫ 1) ≈ 0.123 S m^{-1}. With $\overline{Q}_V{}^0$ = 23.8 × 10^6 C m^{-3}, we obtain $\overline{\sigma}_f{}^0$ ($R \gg 1$) ≈ 1.2 S m^{-1}. Both are very high value indicating that the pore water of shale is always very conductive even when the shale is in contact with an ion depleted electrolyte.

[39] The macroscopic current density and its contributions are

$$\mathbf{J} = \phi\overline{\mathbf{J}} = -\sigma_0\nabla\psi \quad (86)$$

$$\mathbf{J}_{(\pm)} = \phi\overline{\mathbf{J}}_{(\pm)} = -\sigma^0_{(\pm)}\nabla\psi, \quad (87)$$

where σ_0 is the DC electrical conductivity of the porous shale (in the thermostatic state) and $\sigma^0_{(\pm)}$ represent the contributions to σ_0 ($\sigma_0 = \sigma^0_{(+)} + \sigma^0_{(-)}$). It follows that we have

$$\sigma_0 = \overline{\sigma}^0_f/F \quad (88)$$

$$\sigma^0_{(\pm)} = \overline{\sigma}^0_{(\pm)}/F = C^0_f e\beta_{(\pm)}\left(\sqrt{R^2+1} + (\pm 1)R\right)/F. \quad (89)$$

Equation (88) can also be obtained directly from the differential effective medium theory assuming that the porous material is composed of insulating grains immersed in a continuous fluid of conductivity $\overline{\sigma}_f{}^0$. Such type of analysis yields $F = \phi^{-m}$, where the cementation exponent m can be related to the shape distribution of the grains [*Mendelson and Cohen*, 1982].

[40] We introduce the Hittorf numbers $T^0_{(\pm)}$ for the cations and the anions. The Hittorf numbers represent the fraction of electrical current transported by the cations and anions in the pore water of the shale. This definition immediately yields

$$T^0_{(\pm)} \equiv \frac{\sigma^0_{(\pm)}}{\sigma_0} \quad (90)$$

$$T^0_{(\pm)} \equiv \frac{\beta_{(\pm)}\left(\sqrt{R^2+1} + (\pm 1)R\right)}{\left[\left(R + \sqrt{R^2+1}\right)\beta_{(+)} + \left(-R + \sqrt{R^2+1}\right)\beta_{(-)}\right]}, \quad (91)$$

with the property $T^0_{(+)} + T^0_{(-)} = 1$, $0 \leq T^0_{(\pm)} \leq 1$, in the limit $R \gg 1$, $T^0_{(\pm)} = 0$, and in the limit $R = 0$, $T^0_{(\pm)} = t_{(\pm)}$ where $t_{(\pm)}$ are the Hittorf numbers of the ions of the brine in the reservoir in contact with the shale. They are defined by $t_{(\pm)} = \beta_{(\pm)}/(\beta_{(+)} + \beta_{(-)})$ [*MacInnes*, 1961].

[41] Finally, the components L_{11} and L_{22} of $\mathbf{L}$ in equation (42) are

$$L_{11} = \sigma^0_{(+)}/e^2, \quad (92)$$

$$L_{22} = \sigma^0_{(-)}/e^2. \quad (93)$$

Note that in the modeling of surface conductivity, we have not accounted for the contribution of the Stern layer. This is

because this contribution, while being important at a frequency of few kilohertz where electrical conductivity measurements are usually performed, could be essentially negligible in the DC domain [e.g., *Arulanandan*, 1969].

4.2. Permeability

[42] The Darcy filtration velocity is obtained by volume averaging the local water velocity $\mathbf{v}_f$ in the connected pore space:

$$\mathbf{U} = \frac{1}{V}\int_{V_p} \mathbf{v}_f dV_p. \tag{94}$$

The pore fluid velocity $\mathbf{v}_f$ and the effective pore fluid pressure $\overline{p}$ (which encapsulates the gravity and osmotic contributions) are local functions of the position $\mathbf{r}$ in the connected pore space. They are related to the macroscopic fluid pressure gradient by [*Pride*, 1994]

$$\mathbf{v}_f(\mathbf{r}) = \frac{\mathbf{g}(\mathbf{r})}{\eta_f}\frac{\Delta\overline{p}}{H} \tag{95}$$

$$\overline{p}(\mathbf{r}) = h(\mathbf{r})\frac{\Delta\overline{p}}{H}. \tag{96}$$

The local Stokes equation (66) reduces to $\eta_f \nabla^2\mathbf{v}_f = \nabla\overline{p}$. Equations (67), (95), and (96) yield

$$\nabla^2\mathbf{g} = \nabla h, \mathbf{r} \in V_p, \tag{97}$$

$$\nabla\cdot\mathbf{g} = 0, \mathbf{r} \in V_p, \tag{98}$$

$$\mathbf{g} = 0, \mathbf{r} \in S_w, \tag{99}$$

and the field $\mathbf{g}$ and h are null in the matrix. From equations (94) and (97)–(99) the Darcy filtration velocity is governed by the Darcy's law:

$$\mathbf{U} = -\frac{k}{\eta_f}\nabla\overline{p} \tag{100}$$

$$k = -\frac{1}{V}\int_{V_p} \hat{\mathbf{z}}.\mathbf{g}(\mathbf{r})dV_p. \tag{101}$$

The permeability can be also determined by averaging the viscous dissipation of energy in the pore fluid. This yields the representation formula $k = \langle\overline{\overline{\sigma}}_f^V : \overline{\overline{\sigma}}_f^V\rangle/(\Delta p/H)^2$ where angle brackets represent the volume average given by equation (29), $\overline{\overline{\sigma}}_f^V$ is the viscous contribution to the Cauchy stress tensor of the pore fluid (see equation (54)), and the colon indicates a tensor dot product ($\mathbf{a}:\mathbf{b} = a_{ij}b_{ij}$ with the Einstein convention). The coefficient L_{33} of $\mathbf{L}$ in equation (42) is

$$L_{33} = \frac{k}{\eta_f}. \tag{102}$$

By replacing the boundary condition (101) by the less restrictive one $\mathbf{n}\cdot\mathbf{g} = 0, \mathbf{r} \in S_w$ (implying $\mathbf{g} \neq 0, \mathbf{r} \in S_w$), *Pride* [1994] obtained an approximate expression relating the DC permeability to a characteristic pore length Λ and to the electrical formation factor F (defined by equation (81)),

$$k \approx \frac{\Lambda^2}{8F} \tag{103}$$

$$\Lambda = 2\frac{\int_V |\nabla\Gamma|^2 dV_p}{\int_{S_w} |\nabla\Gamma|^2 dS}, \tag{104}$$

where Γ is solution of the boundary value problem (73)–(75). The parameter Λ, introduced by *Johnson et al.* [1987] is a weighted pore volume-to-surface ratio that provides a measure of the dynamically connected part of the pore network [*Avellaneda and Torquato*, 1991; *Kostek et al.*, 1992]. For a network of capillaries of radius R, $\Lambda = R$. For a granular material with grain diameter d, *Revil and Cathles* [1999] obtained $\Lambda = d/2m(F-1)$, where $F = \phi^{-m}$ is the electrical formation factor. The length scale Λ is also closely related to the characteristic pore throat diameter l_c determined from mercury intrusion and percolation concepts by $l_c/2\Lambda \approx 2.66$ [*Wong*, 1994].

4.3. Thermal Conductivity

[43] In absence of any driving forces other than the application of a thermal gradient between the two reservoirs, the macroscopic heat flux is obtained by volume averaging the local heat flux,

$$\mathbf{H} \equiv \frac{1}{V}\left[\int_{V_p} \mathbf{h}dV_p + \int_{V_g} \mathbf{h}dV_g\right] = -\lambda\nabla T, \tag{105}$$

where λ is the thermal conductivity of the water-saturated porous shale. The boundary conditions for the thermal conductivity problem are given by *Revil* [2000, and references therein]. A simple phase average yields $L_{44} = \lambda = (1-\phi)\lambda_g + \phi\lambda_f$, where λ_g and λ_f are the thermal conductivities of the grains and pore fluid, respectively. Despite the fact that this expression works rather well, a more precise relationship is sometimes needed. *Revil* [2000] derived an equation for the effective thermal conductivity of a water-saturated granular composite based on the differential effective medium approach

$$\lambda = \frac{\lambda_f}{f}\left[f\,\Theta + \frac{1}{2}(1-\Theta)\left(1-\Theta+\sqrt{(1-\Theta)^2+4f\,\Theta}\right)\right] \tag{106}$$

$$f \equiv \phi^{\frac{m}{1-m}}. \tag{107}$$

where the dimensionless number $\Theta \equiv \lambda_g/\lambda_f$ is the ratio between the thermal conductivity of the grain to the thermal conductivity of the pore fluid and m is the electrical cementation exponent. The dimensionless parameter f is a "thermal formation factor" for the thermal conductivity problem. It is related to the electrical formation factor F by

$f = F^{1/(m-1)}$ [*Revil*, 2000]. Equation (106) is equivalent to a single phase average only if $m \approx 2$.

4.4. Summary of the Key Parameters

[44] The influence of the texture upon the evaluation of the four conductivity terms depends on three independent properties, the porosity ϕ, the cementation exponent m (m and ϕ allow to determine the electrical and thermal formation factors, F and f), and the length scale Λ. In addition, the effective charge per unit pore volume $\overline{Q}_V{}^0$ plays a critical role in the electrical conductivity problem. In section 5 we show that no other textural parameters are needed to evaluate the influence of the texture upon the coupling terms.

5. Coupling Terms

[45] We determine now the 12 coupling terms (six terms if Onsager reciprocity holds). The first assumption made here is related to the interdependency of ionic transport inside the connected pore volume except for electrical coupling. In other words, there is no diffusion flux of ionic species that is not controlled by solvent transfer. This leads directly to

$$L_{12} = L_{21} = 0 \tag{108}$$

in equation (42). This assumption is valid in the dilute case <0.1 mol L^{-1} [e.g., *Newman*, 1967].

[46] We turn our attention to the determination of the ionic flux densities associated with fluid flow under a fluid pressure gradient (electrokinetic contributions). We consider $\mathbf{v}_f = 0$ at the interface between the Stern and the Gouy-Chapman diffuse layers. So only the ions contained in the Gouy-Chapman diffuse layer are dragged along with the flux of the pore water. The fluid pressure gradient is considered to be the unique driving force here and again we linearize the flux. This yields

$$\mathbf{J}_{(\pm)} = \frac{1}{V}\int_{V_p} \overline{C}_{(\pm)}\mathbf{v}_f dV_p, \tag{109}$$

$$\mathbf{J}_{(\pm)} = \frac{\overline{C}^0_{(\pm)}}{V}\int_{V_p} \mathbf{v}_f dV_p, \tag{110}$$

$$\mathbf{J}_{(\pm)} = -\frac{k}{\eta_f}\overline{C}^0_{(\pm)}\nabla\overline{p}, \tag{111}$$

$$L_{13} = \frac{k}{\eta_f}\overline{C}^0_{(+)}, \tag{112}$$

$$L_{23} = \frac{k}{\eta_f}\overline{C}^0_{(-)}. \tag{113}$$

[47] The conjugated effect is called electro-osmosis. The electro-osmotic flow is obtained by volume averaging the local Stokes equation with a source term associated with the free charge density of the pore space:

$$\left\langle \eta_f \nabla^2 \mathbf{v}_f \right\rangle = \left\langle \overline{Q}^0_V \mathbf{E} \right\rangle. \tag{114}$$

We rewrite the local fluid velocity as the sum of two contributions, one is associated with the cations and the other to the anions. We assume that the movement of cations and anions are independent of each other except through the influence of the electrical field, so $\mathbf{v}_f = \mathbf{v}_{(+)} + \mathbf{v}_{(-)}$ and

$$\left\langle \eta_f \nabla^2 \mathbf{v}_{(\pm)} \right\rangle = \left\langle \pm e\overline{C}_{(\pm)}\mathbf{E} \right\rangle. \tag{115}$$

Using equations (36) and (37) and using the fact that in the thermostatic state $\langle \mathbf{E}_f{}^0 \rangle = 0$, we obtain

$$\left\langle \eta_f \nabla^2 \mathbf{v}_{(\pm)} \right\rangle = \pm e\overline{C}^0_{(\pm)}\langle \mathbf{e}_f \rangle, \tag{116}$$

where we have kept only first-order perturbations in the product of the state variables. The pore fluid velocities $\mathbf{v}_{(\pm)}$ and the local electrical potential ψ are local functions of the position $\mathbf{r}$ in the connected pore space:

$$\mathbf{v}_{(\pm)}(\mathbf{r}) = \frac{\mathbf{g}_{(\pm)}(\mathbf{r})}{\eta_f}\frac{\Delta\psi}{H} \tag{117}$$

$$\psi(\mathbf{r}) = \Gamma(\mathbf{r})\frac{\Delta\psi}{H}, \tag{118}$$

where the functions $\mathbf{g}_{(\pm)}(\mathbf{r})$ obey the following boundary value problem

$$\nabla^2 \mathbf{g}_{(\pm)} = \pm e\overline{C}^0_{(\pm)}\nabla\Gamma, \mathbf{r} \in V_p, \tag{119}$$

$$\nabla \cdot \mathbf{g}_{(\pm)} = 0, \mathbf{r} \in V_p, \tag{120}$$

$$\mathbf{n}.\mathbf{g}_{(\pm)} = 0, \mathbf{r} \in S_w. \tag{121}$$

Note that the boundary conditions (121) are consistent with the use of the approximation leading to equation (103). This yields

$$\mathbf{U}_{(\pm)} = \frac{\pm e\overline{C}^0_{(\pm)}}{\eta_f}\left\langle \hat{\mathbf{z}}.\mathbf{g}_{(\pm)}(\mathbf{r}) \right\rangle \nabla\psi. \tag{122}$$

The net filtration velocity of the brine is obtained by $\mathbf{U} = \mathbf{U}_{(+)} + \mathbf{U}_{(-)}$. This yields $\mathbf{U} = -(\overline{Q}_V{}^0 k/\eta_f)\nabla\psi$. As $\mathbf{U}_{(+)} = L_{31}\nabla\tilde{\mu}_{(+)}$ and $\mathbf{U}_{(-)} = L_{32}\nabla\tilde{\mu}_{(-)}$ in equation (42), we obtain

$$L_{31} = \frac{k}{\eta_f}\overline{C}^0_{(+)} \tag{123}$$

$$L_{32} = \frac{k}{\eta_f}\overline{C}^0_{(-)}. \tag{124}$$

Comparison between equations (112), (113), (123), and (124) shows that $L_{13} = L_{31}$, $L_{23} = L_{32}$.

[48] We determine now the terms L_{41} and L_{42} in equation (42). Thermal diffusion and the "diffusional thermoeffect" result from the coupling between ionic and heat transport in the pore water of the shale. The underlying physics of this coupling is related to the relative motion of ions associated with a change in the local intensity of the intermolecular forces. The adjustment occasioned by such relative motion of the ions also result in a finite heat effect. We consider here the case of a solute ion transported from reservoir II at temperature T to reservoir I at temperature T_0 in a stationary solvent. In this case, a quantity of heat is absorbed from reservoir II corresponding to the heat $Q_{(\pm)}$ transported by the ions (Dufour effect). The heat flux associated with migration of anions and cations in a stationary solvent is approximately given by

$$\mathbf{H} = Q_{(+)}\mathbf{J}_{(+)} + Q_{(-)}\mathbf{J}_{(-)} \tag{125}$$

$$\mathbf{H} = -\frac{Q_{(+)}\sigma^0_{(+)}}{e^2}\nabla\tilde{\mu}_{(+)} - \frac{Q_{(-)}\sigma^0_{(-)}}{e^2}\nabla\tilde{\mu}_{(-)}, \tag{126}$$

and $L_{41} = \sigma^0_{(+)}Q_{(+)}/e^2$ and $L_{42} = \sigma^0_{(-)}Q_{(-)}/e^2$ in equation (42).

[49] The symmetrical effect is called thermodiffusion or Soret effect. The macroscopic ionic densities are given by $\mathbf{J}_{(\pm)} = \langle \mathbf{j}_{(\pm)} \rangle$, and therefore

$$\mathbf{J}_{(\pm)} = -\frac{1}{V}\int_{V_p}\left(\frac{\beta_{(\pm)}\overline{C}_{(\pm)}}{eT_0}Q_{(\pm)}\nabla T\right)dV_p \tag{127}$$

$$\mathbf{J}_{(\pm)} = -\frac{\sigma^0_{(\pm)}Q_{(\pm)}}{e^2T_0}\nabla T + \ldots, \tag{128}$$

keeping again only first-order terms. Onsager reciprocity is again satisfied ($L_{14} = L_{41}$, $L_{24} = L_{42}$).

[50] The last coupling terms to define are the coefficients L_{34} and L_{43} in equation (42). The heat flow associated with the application of a fluid pressure gradient applied between the two reservoirs is proportional to the flux of matter. The proportionality coefficient corresponds to the heat transferred by unit mass. It is called the "heat of transfer of the thermomechanical effect" (note, however, that this expression should be avoided because, strictly speaking, there is no mechanical effect involved here). The heat flux is carried along with pore water during transport of the solvent through the porous material:

$$\mathbf{H} = \frac{1}{V}\int_{V_p} Q_f\mathbf{v}_f dV_p, \tag{129}$$

$$\mathbf{H} \approx \frac{Q_f}{V}\int_{V_p}\mathbf{v}_f dV_p, \tag{130}$$

$$\mathbf{H} = -\frac{Q_f k}{\eta_f}\nabla\overline{p}, \tag{131}$$

where we have used equations (94), (100), and (101). This yields $L_{43} = Q_f k/T_0\eta_f$ for the thermomechanical coefficient.

[51] The conjugated effect is called thermo-osmosis. In thermo-osmosis the driving force is a temperature gradient between the two reservoirs. This temperature gradient causes the ions to migrate, setting up a flow of the solvent through viscous coupling. Volume averaging the Stokes equation yields

$$\left\langle \eta_f\nabla^2\mathbf{v}_f \right\rangle = \left\langle Q_f\nabla T/T_0 \right\rangle. \tag{132}$$

The pore fluid velocity $\mathbf{v}_f$ and the pore fluid temperature T are local functions of the position $\mathbf{r}$ in the connected pore space:

$$\mathbf{v}(\mathbf{r}) = \frac{\mathbf{g}(\mathbf{r})}{\eta_f}\frac{\Delta T}{H} \tag{133}$$

$$T(\mathbf{r}) = \Gamma(\mathbf{r})\frac{\Delta T}{H}, \tag{134}$$

and the vector $\mathbf{g}(\mathbf{r})$ obeys to

$$\nabla^2\mathbf{g}(\mathbf{r}) = \left(Q_f/T_0\right)\nabla\Gamma, \mathbf{r} \in V_p, \tag{135}$$

$$\nabla\cdot\mathbf{g}(\mathbf{r}) = 0, \mathbf{r} \in V_p, \tag{136}$$

$$\mathbf{n}.\mathbf{g} = 0, \mathbf{r} \in S_w. \tag{137}$$

Note that the boundary conditions (137) are consistent with the approximation (103). This yields

$$\mathbf{U} = \frac{Q_f}{\eta_f T_0}\langle \hat{\mathbf{z}}.\mathbf{g}(\mathbf{r})\rangle\nabla T \tag{138}$$

$$\mathbf{U} \approx \frac{Q_f k}{\eta_f T_0}\nabla T, \tag{139}$$

and therefore $L_{34} = Q_f k/T_0\ \eta_f = \rho_f C_v^f k/\eta_f$ and $L_{34} = L_{43}$. The term L_{34} is called the thermo-osmotic coefficient.

6. Final Form of the Constitutive Equations

[52] An explicit form of the phenomenological linear flux force equations and the macroscopic continuity equations is

$$\begin{bmatrix}\mathbf{J}_{(+)}\\ \mathbf{J}_{(-)}\\ \mathbf{U}\\ \mathbf{H}\end{bmatrix} = -\mathbf{L}\begin{bmatrix}\nabla\tilde{\mu}_{(+)}\\ \nabla\tilde{\mu}_{(-)}\\ \nabla\overline{p}\\ \nabla T/T_0\end{bmatrix} \tag{140}$$

$$\nabla\cdot\begin{bmatrix}M_{(+)}\mathbf{J}_{(+)}\\ M_{(+)}\mathbf{J}_{(-)}\\ \rho_f\mathbf{U}\\ \mathbf{H}\end{bmatrix} = -\frac{\partial}{\partial t}\begin{bmatrix}M_{(+)}\overline{C}_{(+)}\phi\\ M_{(-)}\overline{C}_{(-)}\phi\\ \rho_f\phi\\ \rho C_v T\end{bmatrix} + \begin{bmatrix}M_{(+)}R_{(+)}\\ M_{(-)}R_{(-)}\\ \rho_f F\\ Q_S\end{bmatrix}, \tag{141}$$

where $M_{(\pm)} = \rho_{(\pm)}\ \Omega_{(\pm)}$ are the molecular weight of the ions, C_v is the specific heat (per unit mass) of the porous shale (in J kg^{-1} K^{-1}), $R_{(\pm)}(\mathbf{r})$ are the production rates of cations and

anions per unit volume of the porous shale (in mol m^{-3} s^{-1}), Q_S is the source term per unit mass for heat, and $F(\mathbf{r})$ represents the volumetric bulk production rate of the pore fluid (water plus ions) per unit total volume (in s^{-1}) ($F(\mathbf{r})$ is positive in the case of injection and negative in the case of abstraction). The matrix $\mathbf{L}$ is given by

$$\mathbf{L} = \begin{bmatrix} \frac{\sigma^0_{(+)}}{e^2} & 0 & \overline{C}^0_{(+)}\frac{k}{\eta_f} & \frac{\sigma^0_{(+)}}{e^2}Q_{(+)} \\ 0 & \frac{\sigma^0_{(-)}}{e^2} & \overline{C}^0_{(-)}\frac{k}{\eta_f} & \frac{\sigma^0_{(-)}}{e^2}Q_{(-)} \\ \overline{C}^0_{(+)}\frac{k}{\eta_f} & \overline{C}^0_{(-)}\frac{k}{\eta_f} & \frac{k}{\eta_f} & \frac{k}{\eta_f}\rho_f C^f_v \\ \frac{\sigma^0_{(+)}}{e^2}Q_{(+)} & \frac{\sigma^0_{(-)}}{e^2}Q_{(-)} & \frac{k}{\eta_f}\rho_f C^f_v & \lambda T_0 \end{bmatrix}. \quad (142)$$

Now that the petrophysical model for the full set of the material properties is complete, we proceed in the next section to an application to brine filtration and diffusion processes through shales. An alternative form of the constitutive equations is discussed in Appendix A.

7. Filtration and Diffusion Efficiencies

[53] It has been known for a long time that rocks containing large amounts of clay minerals exhibit permselective brine filtration properties [e.g., *Russel*, 1933; *Hanshaw and Coplen*, 1973]. As a result of anion (and sometimes cation) depletion from the connected porosity, the effluent is observed to be less saline than the original solution entering the clay-rich material. This property of clay-rich rocks has receive several names in the literature like salt filtering, reverse or negative osmosis, hyperfiltration or ultrafiltration (Figure 3). This process could influence partly salinity profiles in siliciclastic-filled sedimentary basins like in the Gulf Coast of Mexico.

[54] In isothermal conditions a straight application of the model developed in section 6 yields

$$\mathbf{J}_{(\pm)} = -(\pm 1)\frac{\sigma^0_{(\pm)}}{e}\nabla\psi - \frac{\sigma^0_{(\pm)}}{e^2}\nabla\mu_{(\pm)} + \overline{C}^0_{(\pm)}\mathbf{U}, \quad (143)$$

where we have neglected the various electro-osmotic contributions occurring in the Darcy filtration velocity in regard to the flux associated with the imposed fluid pressure gradient. The electrical current density is then given by

$$\mathbf{J} = e\left(\mathbf{J}_{(+)} - \mathbf{J}_{(-)}\right) \quad (144)$$

$$\mathbf{J} = -\sigma_0\nabla\psi + \frac{k_b T}{e}\left(\sigma^0_{(-)} - \sigma^0_{(+)}\right)\nabla\ln C_f + \frac{\eta_f L_0}{k}\mathbf{U}. \quad (145)$$

The electrokinetic coefficient L_0 is defined by

$$L_0 = e(L_{13} - L_{23}) = \frac{k}{\eta_f}\left(\overline{C}^0_{(+)} - \overline{C}^0_{(-)}\right) \quad (146)$$

$$L_0 = \frac{\overline{Q}^0_V k}{\eta_f}. \quad (147)$$

The condition $\mathbf{J} = 0$ yields

$$\nabla\psi = \frac{k_b T}{e}\left(T^0_{(-)} - T^0_{(+)}\right)\nabla\ln C_f + \frac{\eta_f L_0}{k\sigma_0}\mathbf{U}, \quad (148)$$

where $T^0_{(\pm)} = \sigma^0_{(\pm)}/\sigma_0$ are the Hittorf numbers of the porous shale layer. They are given by equations (90) and (91). They are therefore controlled by the dimensionless number R only. The electrical field through the shale layer is given by

$$-\nabla\psi = -\frac{k_b T}{e}\left(1 - 2T^0_{(+)}\right)\nabla\ln C_f - \frac{\eta_f L_0}{k\sigma_0}\mathbf{U}. \quad (149)$$

The first contribution corresponds to the membrane potential [*Jin and Sharma*, 1994], while the second contribution corresponds to the streaming potential. Combining equations (143), (145), and (149) yields

$$\mathbf{J}_{(\pm)} = (\mp 1)T^0_{(\pm)}\frac{\eta_f L_0}{ke}\mathbf{U} - \frac{2k_b T\sigma^0_{(\pm)}}{e^2}T^0_{(\mp)}\nabla\ln C_f + \overline{C}^0_{(\pm)}\mathbf{U}. \quad (150)$$

The salt flux through the membrane is defined by

$$\mathbf{J}_d = \frac{1}{2}\left(\mathbf{J}_{(+)} + \mathbf{J}_{(-)}\right) \quad (151)$$

$$\mathbf{J}_d = \frac{1}{2}\left[\left(\overline{C}^0_{(+)} + \overline{C}^0_{(-)}\right)\mathbf{U} + \frac{\eta_f L_0}{ke}\left(T^0_{(-)} - T^0_{(+)}\right)\mathbf{U}\right] - \frac{2k_b T}{e^2}\left(\frac{\sigma^0_{(+)}\sigma^0_{(-)}}{\sigma_0}\right)\nabla\ln C_f. \quad (152)$$

In absence of pore water flow ($\mathbf{U} = 0$ in equation (152)) the diffusion flux is defined by Fick's law

$$\mathbf{J}_d = -D^0_{\text{eff}}\nabla C_f. \quad (153)$$

So by comparing the last term of equation (152) with equation (153), the effective electrodiffusion coefficient of the salt is simply given by

$$D^0_{\text{eff}} = \frac{2k_b T}{e^2 C_f}\left(\frac{\sigma^0_{(+)}\sigma^0_{(-)}}{\sigma^0_{(+)} + \sigma^0_{(-)}}\right), \quad (154)$$

which generalizes the Nernst-Hartley equation of salt diffusivity in electrolytes to charged composites.

[55] From equations (152) to (154) the flux of the salt is given by

$$\mathbf{J}_d = \frac{1}{2}\left[\left(\overline{C}^0_{(+)} + \overline{C}^0_{(-)}\right)\mathbf{U} + \frac{\eta_f L_0}{ke}\left(1 - 2T^0_{(+)}\right)\mathbf{U}\right] - D^0_{\text{eff}}\nabla C_f. \quad (155)$$

The flux of the salt is the sum of two contributions. The first one is related to brine transport associated with the filtration flux, which leads to brine filtration effects. The second is

the diffusion of salt in the salinity gradient. We investigate these two terms separately in sections 7.1 and 7.2.

7.1. Salt Filtration Efficiency

[56] If we assume that the convective flux of salt associated with the solvent transport is much greater than the diffusion of the salt through the porous shale, the flux of salt is

$$\mathbf{J}_d \approx \frac{1}{2}\left[\left(\overline{C}^0_{(+)} + \overline{C}^0_{(-)}\right)\mathbf{U} + \frac{\eta_f L_0}{ke}\left(T^0_{(-)} - T^0_{(+)}\right)\mathbf{U}\right]. \quad (156)$$

The salinity of the effluent $\tilde{C}_f$ is defined by

$$\mathbf{J}_d = \tilde{C}_f \mathbf{U}. \quad (157)$$

Equations (156) and (157) yield

$$\tilde{C}_f = \frac{1}{2}\left[\overline{C}^0_{(+)} + \overline{C}^0_{(-)} + \left(\frac{L_0\eta_f}{ek}\right)\left(T^0_{(-)} - T^0_{(+)}\right)\right] \quad (158)$$

$$\tilde{C}_f = \frac{1}{2}\left[\left(\frac{\overline{Q}_V^{0^2}}{e^2} + 4C_f^2\right)^{1/2} + \left(\frac{L_0\eta_f}{ek}\right)\left(1 - 2T^0_{(+)}\right)\right], \quad (159)$$

using $T^0_{(-)} = 1 - T^0_{(+)}$. Equation (159) provides the fundamental relationship between the concentration of the effluent and the salinity of the brine at the entrance of the shale. According to equation (159), the salinity of the ultrafiltrate is independent of the thickness of the shale layer and independent of the Darcy filtration velocity. It depends on the transport numbers of the ionic species in the porous material. We check two limiting cases. The first case corresponds to an uncharged material, $\overline{Q}_V{}^0 = 0$. This yields $\tilde{C}_f = C_f$; that is, the salinity of the effluent is equal to the salinity of the brine at the entrance of the shale as it should be. The second case is that of a "perfect" membrane with $T^0_{(+)} = 1$ and $T^0_{(-)} = 1 - T^0_{(+)} = 0$ and $\overline{Q}_V{}^0/e \gg C_f$. This yields

$$\lim_{\substack{\overline{Q}_V^0 \gg C_f \\ T^0_{(+)}=1}} \tilde{C}_f = 0. \quad (160)$$

For a perfect membrane, the salinity of the effluent is null. Note that according to the two previous limits, the salt filtration efficiency depends on the salinity of the pore water. The less the salinity of the brine is, the more efficient the salt filtration process. This is in agreement with the experimental results of *Malusis et al.* [2003]. From equation (159), we have

$$\tilde{C}_f = C_f\left[\left(\frac{\overline{Q}_V^{0^2}}{4e^2C_f^2} + 1\right)^{1/2} + \left(\frac{L_0\eta_f}{2ekC_f}\right)\left(1 - 2T^0_{(+)}\right)\right]. \quad (161)$$

The shale filtration efficiency ε is defined by

$$\varepsilon \equiv \frac{C_f - \tilde{C}_f}{C_f} = 1 - \frac{\tilde{C}_f}{C_f}, \quad (162)$$

with $0 \le \varepsilon \le 1$ ($\varepsilon = 1$ corresponds to a perfect membrane). Combining equations (161) and (162) yields

$$\varepsilon = 1 - \left(1 + R^2\right)^{1/2} - R\left(1 - 2T^0_{(+)}\right). \quad (163)$$

The brine filtration efficiency is determined by the transport number $T^0_{(+)}$ (which is a function of R) and the key dimensionless parameter R defined in section 4.1 by equation (83), both being evaluated in the thermostatic state. The model is consistent with experimental data (see Figure 4).

7.2. Salt Diffusivity Efficiency

[57] Assuming now that diffusion is the main mechanism of transport, the diffusive flux is related to the gradient of the brine concentration by an apparent Fick's law, which encapsulates electrostatic effects:

$$\mathbf{J}_d = -D^0_{\text{eff}} \nabla C_f, \quad (164)$$

where D^0_{eff} is given by equation (154). If the shale is uncharged $Q_V = 0$ (e.g., at the point of zero charge), we recover equation (1) of *McDuff and Ellis* [1979]:

$$D^0_{\text{eff}} = \frac{D^f_{\text{eff}}}{F}, \quad (165)$$

$$D^f_{\text{eff}} = \frac{2k_bT}{e}\left(\frac{\beta_{(+)}\beta_{(-)}}{\beta_{(+)} + \beta_{(-)}}\right), \quad (166)$$

$$D^f_{\text{eff}} = \frac{2D^f_{(+)}D^f_{(-)}}{D^f_{(+)} + D^f_{(-)}}, \quad (167)$$

where D^f_{eff} is the (electro) diffusivity of the salt in the brine, $D^f_{(\pm)} = (k_bT/e)\beta_{(\pm)}$ (according to the Nernst-Einstein relationship) are the self-diffusion coefficients of the ions in the brine (e.g., Table 5 for NaCl), and F is the electrical formation factor arising in the electrical conductivity problem. In Table 5 we report the diffusivity of NaCl determined using equation (167) and the values of the self-diffusion coefficients of the ions (Na^+ and Cl^-) in the brine.

[58] Equations (166) or (167) represent various forms of the so-called Nernst-Hartley equation for a 1:1 salt in water. Equation (154), which is nothing else than a macroscopic version of the classical Nernst-Hartley equation, is more general than the models presented by *McDuff and Ellis* [1979] and recently by *Snyder and Marchand* [2001]. Indeed, these models do not account for the membrane behavior of the shale and the influence of the electrical diffuse layer in the DC limit of the electrodiffusion equations. We define an (electro) diffusivity efficiency by

$$\gamma = \frac{D^0_{\text{eff}}}{\lim_{\overline{Q}_V^0 \to 0}\left(D^0_{\text{eff}}\right)} = \frac{D^0_{\text{eff}}}{D^f_{\text{eff}}/F}. \quad (168)$$

The diffusivity efficiency represents therefore the ratio between the effective diffusivity of the salt through the

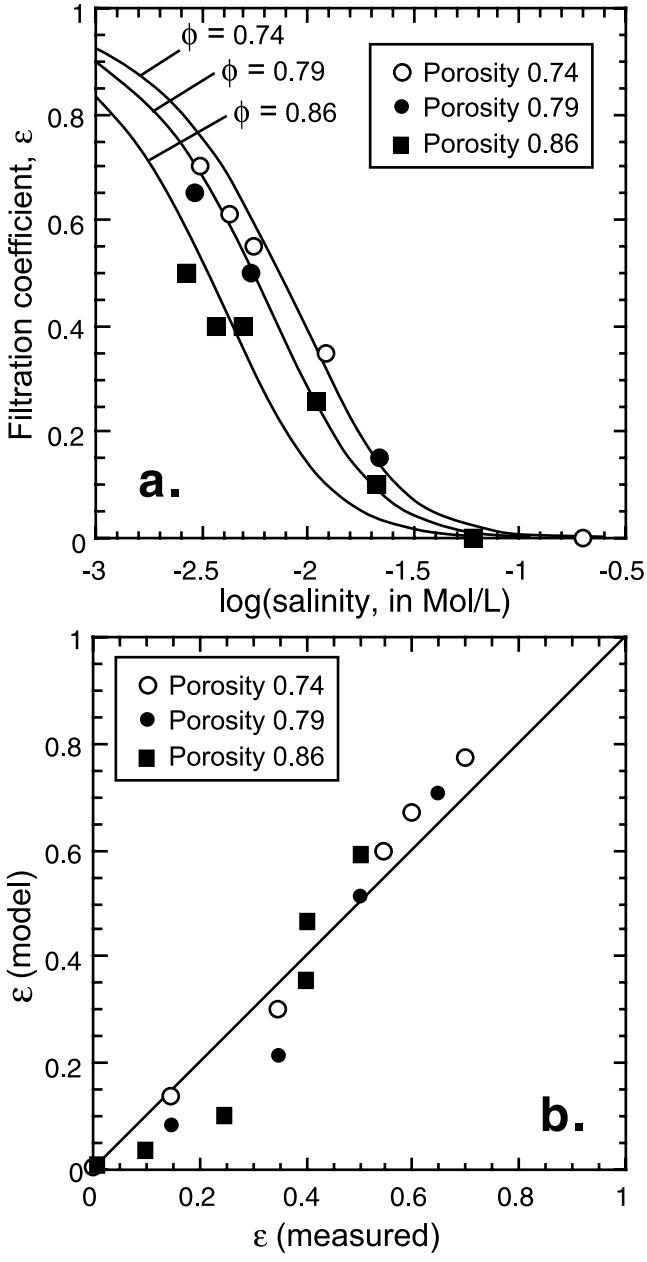

Figure 4. Filtration efficiency. Experimental data from *Malusis et al.* [2003], geosynthetic clay liner, KCl. Parameters used are grain density ρ_g = 2.65 g cm^{-3}, f_Q = 0.94, and CEC = 0.48 meq g^{-1} (measured). Note that the partition coefficient f_Q = 0.94 is consistent with TLM computations (see discussion in section 2.1). Note that the small discrepancy between the model and the experimental data could come from the fact that the partition coefficient is dependent on the ionic strength of the pore water.

porous shale divided by the effective diffusivity that would exist if the porous material would be uncharged. From equation (168) the effective diffusivity is

$$D^0_{\text{eff}} = \frac{D^f_{\text{eff}}}{F}\gamma, \tag{169}$$

where the diffusivity efficiency is obtained from equations (154) and (169):

$$\gamma = F\frac{T^0_{(+)}\left(1-T^0_{(+)}\right)}{t_{(+)}\left(1-t_{(+)}\right)}\frac{\sigma_0}{\sigma^0_f}, \tag{170}$$

$$\gamma = \frac{T^0_{(+)}\left(1-T^0_{(+)}\right)}{t_{(+)}\left(1-t_{(+)}\right)}\frac{\overline{\sigma}^0_f}{\sigma^0_f}, \tag{171}$$

$$\gamma = \frac{\left(\beta_{(+)}+\beta_{(-)}\right)\left(\sqrt{R^2+1}+R\right)\left(\sqrt{R^2+1}-R\right)}{\left(R+\sqrt{R^2+1}\right)\beta_{(+)}+\left(-R+\sqrt{R^2+1}\right)\beta_{(-)}}, \tag{172}$$

where we have used equations (84), (88), (91), and (154) and $T^0_{(\pm)} = \sigma^0_{(\pm)}/\sigma_0$. We have the following limits:

$$\lim_{R\to 0}\gamma = 1 \tag{173}$$

$$\lim_{R\gg 1}\gamma = \frac{1}{t_{(+)}}\left(\frac{1}{2R}\right). \tag{174}$$

Therefore at high salinity, the (electro) diffusivity efficiency is equal to one and the system behaves like an uncharged membrane (by definition of the diffusivity efficiency). At low salinity, the (electro) diffusivity efficiency decreases like $(1/R)$. This means that the shale becomes less and less permeable to the diffusion of the salt when salinity decreases. A comparison between the self-diffusivity coefficient of sodium in a shale ($D^f_{(+)}/F$) and the electrodiffusivity of sodium in a concentration field (equations (169) and (172)) is illustrated in Figure 5. The model predicts that the diffusivity of the salt is smaller for a smaller salinity in qualitative agreement with the experimental results reported by *Malusis and Shackelford* [2002].

8. Concluding Statements

[59] We have developed a model of ionic transport in charged granular porous materials like shales. The model contains a set of new features: (1) The model accounts for the partition of the counterions between the Stern and the Gouy-Chapman layers through the use of a partition coefficient f_Q. (2) New expressions are developed for the electrokinetic properties, Soret and Dufour effects,

Table 5. Diffusivity of NaCl at 25°C[a]

	NaCl, C_f, mol L^{-1}					
	ID[b]	10^{-3}	10^{-2}	10^{-1}	0.5	1
$D^f_{(+)}$ (^{22}Na)[c]	1.33	1.33	1.32	1.29	1.27	1.22
$D^f_{(-)}$ (^{36}Cl)[c]	2.03	1.99	1.97	1.96	1.86	1.78
D^f_{eff} (NaCl)[d]	1.60	1.60	1.58	1.56	1.50	1.44

[a]Diffusivity given in units of $\times$ 10^9 m^2 s^{-1}.
[b]Infinite dilution.
[c]From *Turq et al.* [1969].
[d]From equation (167).

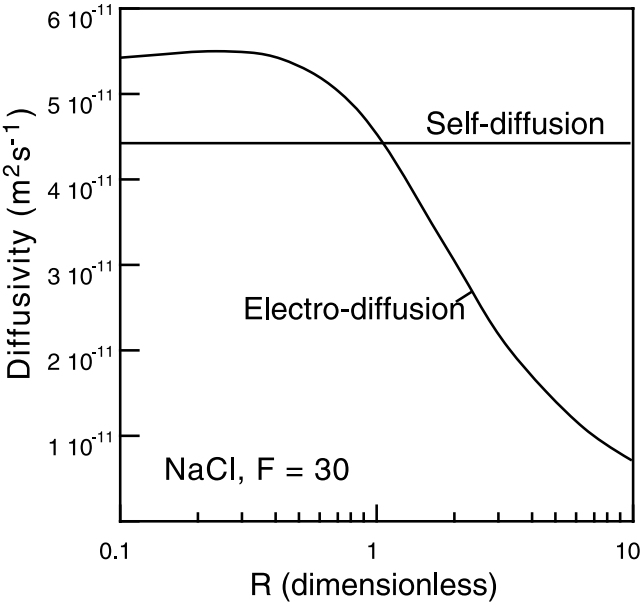

Figure 5. Diffusivity in a shale. Comparison between the self-diffusivity of sodium (we use $F = 30$) and the electrodiffusivity of the salt in a concentration field versus the key dimensionless number R.

electrical conductivity, brine filtration efficiency, and electrodiffusivity in shales. (3) Determination of the material properties entering the constitutive flux equations requires only four well-defined textural parameters (the porosity, the cation exchange capacity, the cementation exponent, and the length scale Λ) plus the partition coefficient f_Q, which can be computed from a triple-layer model of the electrochemical properties of the mineral surface. This makes the model particularly attractive for practical applications.

Appendix A: M Matrix Form of the Constitutive Equations

[60] Another choice of independent fluxes is to consider the electrical current density, the diffusion flux, the Darcy velocity, and the heat flux as independent fluxes. This is actually a very practical choice when regarding what can be easily measured in the laboratory. The electrical current density and the diffusion flux are defined by $\mathbf{J} = e(\mathbf{J}_{(+)} - \mathbf{J}_{(-)})$ and $\mathbf{J}_d = (\mathbf{J}_{(+)} + \mathbf{J}_{(-)})/2$, respectively. This choice lets the dissipation function entering the continuity equation for entropy invariant:

$$D = -2\mathbf{J}_d\nabla\mu_f - \mathbf{J}\nabla\psi - \mathbf{U}\nabla\overline{p} - \mathbf{H}\nabla T/T_0, \qquad (A1)$$

where $\nabla\mu_f = k_bT\nabla\ln C_f$ is the gradient of the chemical potential of the brine. The first term corresponds to the dissipation associated with diffusion, the second term is the Joule dissipation associated with electrical conduction, the third term is a dissipation associated with water flow and viscous friction between the water and the grain skeleton at their common interface, and the last term is a dissipation contribution associated with heat flow through the porous material. So the generalized phenomenological equations are

$$\begin{bmatrix} 2\mathbf{J}_d \\ \mathbf{J} \\ \mathbf{U} \\ \mathbf{H} \end{bmatrix} = -\mathbf{M}\begin{bmatrix} \nabla\mu_f \\ \nabla\psi \\ \nabla\overline{p} \\ \nabla T/T_0 \end{bmatrix}, \qquad (A2)$$

where $\mathbf{M}$ is a 4×4 matrix of material properties. The components obey to the Onsager's reciprocity $M_{ij} = M_{ji}$ and $M_{ij}^2 \leq M_{ii}M_{jj}$ to insure $D \geq 0$. The straight conductivity coefficients M_{ii} are always positive while the cross coefficients can be either positive or negative. The generalized continuity equation associated with the $\mathbf{M}$ form of the constitutive equations is

$$\nabla\cdot\begin{bmatrix} \mathbf{J}_d \\ \mathbf{J} \\ \rho_f\mathbf{U} \\ \mathbf{H} \end{bmatrix} = -\frac{\partial}{\partial t}\begin{bmatrix} C_f\phi \\ Q_V\phi \\ \rho_f\phi \\ \rho C_v T \end{bmatrix} + \begin{bmatrix} (R_{(+)} + R_{(-)})/2 \\ e(R_{(+)} - R_{(-)}) \\ \rho_f F \\ Q_S \end{bmatrix}. \qquad (A3)$$

The $\mathbf{L}$ and $\mathbf{M}$ forms are related through

$$M_{11} = L_{11} + L_{22} = \frac{1}{e^2}\left(\sigma^0_{(+)} + \sigma^0_{(-)}\right) = \frac{\sigma_0}{e^2}, \qquad (A4)$$

$$M_{22} = e^2(L_{11} + L_{22}) = \sigma_0, \qquad (A5)$$

$$M_{33} = L_{33} = k/\eta_f, \qquad (A6)$$

$$M_{44} = T_0^2L_{44} = T_0\lambda, \qquad (A7)$$

$$M_{12} = e(L_{11} - L_{22}) = \frac{1}{e}\left(\sigma^0_{(+)} - \sigma^0_{(-)}\right), \qquad (A8)$$

$$M_{13} = L_{13} + L_{23} = \frac{k}{\eta_f}\left(\overline{C}^0_{(+)} + \overline{C}^0_{(-)}\right), \qquad (A9)$$

$$M_{14} = T_0(L_{14} + L_{24}) = \frac{T_0}{e^2}\left(\sigma^0_{(+)}Q_{(+)} + \sigma^0_{(-)}Q_{(-)}\right), \qquad (A10)$$

$$M_{23} = e(L_{13} - L_{23}) = \frac{ek}{\eta_f}\left(\overline{C}^0_{(+)} - \overline{C}^0_{(-)}\right), \qquad (A11)$$

$$M_{24} = eT_0(L_{14} - L_{24}) = \frac{T_0}{e}\left(\sigma^0_{(+)}Q_{(+)} + \sigma^0_{(-)}Q_{(-)}\right), \qquad (A12)$$

$$M_{34} = T_0L_{34} = \frac{k}{\eta_f}\rho_f T_0 C_v^f. \qquad (A13)$$

A1. Salt Diffusivity

[61] The salt diffusivity D (different from the effective salt electrodiffusivity), is related to the coefficient M_{11} by

$$D = \frac{M_{11}k_bT}{2C_f} = \frac{\sigma_0 k_bT}{2e^2C_f}. \qquad (A14)$$

This is an obvious result when one considers an uncharged membrane. In this case the electrical conductivity of the

porous material is given by $\sigma_0 = \sigma_f/F$, where F is the electrical formation factor and the electrical conductivity of the pore water is given by $\sigma_f \approx 2eC_f\,\beta_f$ (where $\beta_f = (1/2)(\beta_{(+)} + \beta_{(-)})$ is the mean mobility of the salt). The diffusivity of the salt $D_f = \beta_f k_b T/e$ (which does not include electrostatic effects) is related to the mean mobility β_f by a Nernst-Einstein relationship $D_f = \beta_f k_b T/e$. This yields to a well-known result $D = D_f/F$.

A2. Salt Electrodiffusivity

[62] We consider now the electrostatic interaction term in the diffusive equation and we rewrite the combined effect of diffusion and electrostatic interaction as an equivalent Fickian process. Neglecting the effect of pressure and temperature gradients, the diffusion flux and the electrical current density are given by

$$\mathbf{J}_d = -\frac{M_{11}}{2}\nabla\mu_f - \frac{M_{12}}{2}\nabla\psi, \tag{A15}$$

$$\mathbf{J}_d = -D\nabla C_f - \frac{1}{2e}\left(\sigma^0_{(+)} - \sigma^0_{(-)}\right)\nabla\psi, \tag{A16}$$

$$\mathbf{J} = -M_{21}\nabla\mu_f - M_{22}\nabla\psi, \tag{A17}$$

$$\mathbf{J} = -\frac{k_b T}{e}\left(\sigma^0_{(+)} - \sigma^0_{(-)}\right)\nabla \ln C_f - \sigma_0\nabla\psi, \tag{A18}$$

respectively. The condition $\mathbf{J} = 0$ yields to an expression for the so-called membrane potential:

$$\nabla\psi = -\frac{k_b T}{e}\left(T^0_{(+)} - T^0_{(-)}\right)\nabla \ln C_f. \tag{A19}$$

Introducing equation (A19) into equation (A16) yields

$$\mathbf{J}_d = -D\nabla C_f + \frac{k_b T}{2e^2\sigma_0}\left(\sigma^0_{(+)} - \sigma^0_{(-)}\right)^2\nabla \ln C_f. \tag{A20}$$

We define the electrodiffusivity of the salt through the porous medium as

$$\mathbf{J}_d = -D^0_{\text{eff}}\nabla C_f. \tag{A21}$$

After some straightforward algebraic manipulations, it follows that the electrodiffusivity is given by a generalized Nernst-Hartley equation

$$D^0_{\text{eff}} = D - \frac{k_b T}{2e^2 C_f}\frac{\left(\sigma^0_{(+)} - \sigma^0_{(-)}\right)^2}{\sigma_0} \tag{A22}$$

$$D^0_{\text{eff}} = \frac{2k_b T}{e^2 C_f}\left(\frac{\sigma^0_{(+)}\sigma^0_{(-)}}{\sigma^0_{(+)} + \sigma^0_{(-)}}\right). \tag{A23}$$

Usually, the apparent diffusivity measured through a rock sample in steady state conditions is the electrodiffusivity and not the true diffusivity.

A3. Streaming Potential Coupling Coefficient

[63] In isothermal conditions and in absence of concentration gradients, the streaming potential coefficient C (in V Pa^{-1}) is defined by

$$C \equiv \left(\frac{\partial\psi}{\partial p}\right)_{\mathbf{J},\mathbf{H}=0} = -\frac{M_{23}}{\sigma_0} \tag{A24}$$

$$C = -\frac{ek}{\eta_f\sigma_0}\left(\overline{C}^0_{(+)} - \overline{C}^0_{(-)}\right) = -\frac{k\overline{Q}^0_V}{\eta_f\sigma_0}. \tag{A25}$$

The asymptotic developments of the electrical conductivity equation yields the following low salinity limit $\overline{\sigma}_0\,(R \gg 1) = \overline{Q}^0_V\,\beta_{(+)}/F$, where $\beta_{(+)}$ is the mobility of the counterions and F is the electrical formation factor. This yields in the low-salinity limit ($R \gg 1$),

$$C(R \gg 1) = -\frac{kF}{\eta_f\beta_{(+)}}, \tag{A26}$$

where the C is independent of the salinity of the pore water. Taking $k = 10^{-18}$ m^2, $F = 30$, $\eta_f = 10^{-3}$ Pa s, $\beta_{(+)}(Na^+, 25°C) = 5.19 \times 10^{-8}$ m^2 s^{-1} V^{-1} yields $C = -580$ mV MPa^{-1}.

A4. Electro-osmotic Coupling Coefficient

[64] In isothermal condition and in absence of concentration gradients, the streaming potential coefficient C_o (in Pa V^{-1}) is defined by

$$C_o \equiv \left(\frac{\partial p}{\partial\psi}\right)_{\mathbf{U},\mathbf{H}=0} = -\frac{M_{32}}{M_{33}} = -\overline{Q}^0_V. \tag{A27}$$

where $\overline{Q}^0_V$ is the excess of charge per unit pore volume of the porous medium in the reference state. So the measurement of the electro-osmotic pressure provides a direct way to evaluate $\overline{Q}^0_V$. Taking $\overline{Q}^0_V = 2 \times 10^6$ C m^{-3} yields an electro-osmotic coupling coefficient equal to 2 MPa V^{-1}. So the electro-osmotic coupling is extremely efficient in shales.

A5. Thermo-osmotic Permeability

[65] The thermo-osmotic permeability k_T (in m^2 s^{-1} K^{-1}) is defined by $\mathbf{U} = -k_T\nabla T$ with all the other thermodynamic forces being negligible. Consequently, using the expression of the matrix $\mathbf{M}$, we have $k_T = M_{34}/T_0 = (k\rho_f/\eta_f)C^f_v$. Taking $k = 10^{-18}$ m^2, $\rho_f = 1000$ kg m^{-3}, $\eta_f = 10^{-3}$ Pa s, and a specific heat per unit mass of water $C^f_v = 4200$ J kg^{-1} $°C^{-1}$, yields $k_T = 10^{-9}$ m^2 s^{-1} K^{-1}. This can be compared with the value $k_T = 2.25 \times 10^{-10}$ m^2 s^{-1} K^{-1} measured by *Shrivastava and Avasthi* [1975] on a kaolinite with a porosity of 0.5 at the average temperature $T = 38.4°C$.

[66] **Acknowledgments.** This work is supported by the French National Research Council (CNRS), the GDR-FORPRO (Research action GDR FORPRO contribution FORPRO 2003/16A), and the French National Agency for Radioactive Waste management (ANDRA). Bruno Hamelin and Joël Lancelot are particularly thanked for their strong supports at CEREGE and through the GDR FORPRO, respectively. The grant of Philippe Leroy

is supported by ANDRA. Daniel Coelho and Scott Altmann (ANDRA) are thanked for their financial support and scientific advices regarding this work. We thank also Françoise and Bernard Angeletti for their support.

References

Arulanandan, K. (1969), Hydraulic and electrical flows in clays, *Clays Clay Miner.*, *17*, 63–76.

Avellaneda, M., and S. Torquato (1991), Rigorous link between fluid permeability, electrical conductivity, and relaxation times for transport in porous media, *Phys. Fluids A*, *3*, 2529–2540.

Avena, M. J., and C. P. De Pauli (1998), Proton adsorption and electrokinetics of an Argentinean Montmorillonite, *J. Colloid Interface Sci.*, *202*, 195–204.

Bercovici, D., Y. Ricard, and G. Shubert (2001), A two-phase model for compaction and damage. 1. General theory, *J. Geophys. Res.*, *106*, 8887–8906.

Besseling, N. A. M. (1997), Theory of hydration forces between surfaces, *Langmuir*, *13*, 2113–2122.

Chu, S.-Y., G. Sposito, and W. A. Jury (1983), The cross-coupling transport coefficient for the steady flow of heat in soil under a gradient of water content, *Soil Sci. Soc. Am. J.*, *47*, 21–25.

De Groot, S. R., and P. Mazur (1984), *Non-equilibrium Thermodynamics*, 510 pp., Dover, Mineola, N. Y.

Gier, S. (1998), Burial diagenetic processes and clay mineral formation in the molasse zone of upper Austria, *Clays Clay Miner.*, *6*, 658–669.

Gu, W. Y., W. M. Lai, and V. C. Mow (1997), A triphasic analysis of negative osmotic flows through charged hydrated soft tissues, *J. Biomech.*, *30*, 71–78.

Hanshaw, B. B., and T. B. Coplen (1973), Ultrafiltration by a compacted clay membrane. II. Sodium ion exclusion at various ionic strengths, *Geochim. Cosmochim. Acta*, *37*, 2311–2327.

Howes, F. A., and S. Whitaker (1985), The spatial averaging theorem revisited, *Chem. Eng. Sci.*, *40*, 1387–1392.

Jin, M., and M. M. Sharma (1994), Shaly sand formation evaluation using a single membrane potential measurement, *J. Pet. Sci. Eng.*, *11*, 301–310.

Johnson, D. L., J. Koplik, and R. Dashen (1987), Theory of dynamic permeability and tortuosity in fluid-saturated porous media, *J. Fluid Mech.*, *176*, 379–402.

Kedem, O., and A. Katchalsky (1961), A physical interpretation of the phenomenological coefficients of membrane permeability, *Trans. Faraday Soc.*, *45*, 143–179.

Kostek, S., L. M. Schwartz, and D. L. Johnson (1992), Fluid permeability in porous media: Comparison of electrical estimates with hydrodynamical calculations, *Phys. Rev. B*, *45*, 186–195.

Lai, W. M., J. S. Hou, and V. C. Mow (1991), A triphasic theory for the swelling and deformation behaviors of articular cartilage, *J. Biomech. Eng.*, *113*, 245–258.

Leroy, P., and A. Revil (2004), A triple layer model of the surface electrochemical properties of clay minerals, *J. Colloids Interface Sci.*, *270*(2), 371–380.

Lin, J.-L. (1991), Thermal diffusion in Liquids, in *Measurements of the Transport Properties of Fluids*, vol. III, *Experimental Thermodynamics*, edited by W. A. Wakeham, A. Nagashima, and J. V. Sengers, pp. 329–354, Blackwell Sci., Malden, Mass.

Lipsicas, M. (1984), Molecular and surface interactions in clay intercalates, in *Physics and Chemistry of Porous Media*, edited by D. L. Johnson and P. N. Sen, pp. 191–202, Am. Inst. of Phys., College Park, Md.

Lockhart, N. C. (1980), Electrical properties and the surface characteristics and structure of clays, II, Kaolinite: A nonswelling clay, *J. Colloid Interface Sci.*, *74*, 520–529.

Ma, C., and R. A. Eggleton (1999), Cation exchange capacity of kaolinite, *Clays Clay Miner.*, *47*, 174–180.

MacInnes, D. A. (1961), *The Principles of Electrochemistry*, 478 pp., Dover, Mineola, N. Y.

Malusis, M. A., and C. D. Shackelford (2002), Coupling effects during steady-state solute diffusion through a semipermeable clay membrane, *Environ. Sci. Technol.*, *36*, 1312–1319.

Malusis, M. A., C. D. Shackelford, and H. W. Olsen (2003), Flow and transport through clay membrane barriers, *Eng. Geol.*, *70*, 235–248.

McDuff, R. E., and R. A. Ellis (1979), Determining diffusion coefficients in marine sediments: A laboratory study of the validity of resistivity techniques, *Am. J. Sci.*, *279*, 666–675.

Mendelson, K. S., and M. H. Cohen (1982), The effect of grain anisotropy on the electrical properties of sedimentary rocks, *Geophysics*, *47*, 257–263.

Meyer, K. H., and J. F. Sievers (1936), La perméabilité des membranes. I. Théorie de la perméabilité ionique, *Helv. Chem. Acta*, *19*, 649.

Michaeli, I., and O. Kedem (1961), Description of the transport of solvent and ions through membranes in terms of differential coefficients. Part I. Phenomenological characterization of flows, *Trans. Faraday Soc.*, *57*, 1185–1190.

Moyne, C., and M. A. Murad (2002), Electro-chemo-mechanical couplings in swelling clays derived from micro/macro-homogeneization procedure, *Int. J. Solids Struct.*, *39*, 6159–6190.

Nernst, W. (1888), Zur kinetic der lösung befindlichen körper: Theorie der diffusion, *Z. Phys. Chem.*, *3*, 613–637.

Newman, J. (1967), Transport processes in electrolytic solutions, *Adv. Electrochem. Electrochem. Eng.*, *5*, 87–136.

Patchett, J. G. (1975), An investigation of shale conductivity, paper presented at SPWLA 16th Annual Logging Symposium, Paper V, 40 pp., Soc. of Prof. Well Log Anal., New Orleans, La., 4–7 June .

Planck, M. (1890), Ueber die erregung von elektricität und wärme in elektrolyten, *Ann. Phys. Chem. Neue Folge*, *39*, 161–186.

Pride, S. (1994), Governing equations for the coupled electromagnetics and acoustics of porous media, *Phys. Rev. B*, *50*, 15,678–15,696.

Revil, A. (1999), Ionic diffusivity, electrical conductivity, membrane and thermoelectric potentials in colloids and granular porous media: A unified model, *J. Colloid Interface Sci.*, *212*, 503–522.

Revil, A. (2000), Thermal conductivity of unconsolidated sediments with geophysical applications, *J. Geophys. Res.*, *105*, 16,749–16,768.

Revil, A., and L. M. Cathles (1999), Permeability of shaly sands, *Water Resour. Res.*, *35*, 651–662.

Revil, A., and P. Leroy (2001), Hydroelectric coupling in a clayey material, *Geophys. Res. Lett.*, *28*, 1643–1646.

Russel, W. L. (1933), Subsurface concentration of chloride brines, *AAPG Bull.*, *17*, 1213–1228.

Shainberg, I., N. Alperovitch, and R. Keren (1988), Effect of magnesium on the hydraulic conductivity of Na-smectite-sand mixtures, *Clays Clay Miner.*, *36*, 432–438.

Shrivastava, R. C., and P. K. Avasthi (1975), Non-equilibrium thermodynamics of thermo-osmosis of water through kaolinite, *J. Hydrol.*, *24*, 111–120.

Sinitsyn, V. A., S. U. Aja, D. A. Kulik, and S. A. Wood (2000), Acid-base surface chemistry and sorption of some lanthanides on K^+-saturated Marblehead illite. I. Results of an experimental investigation, *Geochim. Cosmochim. Acta*, *64*, 185–194.

Slaterry, J. C. (1981), *Momentum, Energy and Mass Transfer in Continua*, Krieger, New York.

Snyder, K. A., and J. Marchand (2001), Effect of speciation on the apparent diffusion coefficient in no-reactive porous system, *Cement Concrete Res.*, *31*, 1837–1845.

Su, Q., Q. Feng, and Z. Shang (2000), Electrical impedance variation with water saturation in rock, *Geophysics*, *65*, 68–75.

Teorell, T. (1935), An attempt to formulate a quantitative theory of membrane permeability, *Proc. Soc. Exp. Biol. Med.*, *33*, 282.

Turq, P., F. Lantelme, and M. Chemla (1969), Coefficients d'auto-diffusion dans les solution acqueuses de NaF et de NaCl, *Electrochim. Acta*, *14*, 1081–1088.

Wong, P. (1994), Flow in porous media: Permeability and displacement patterns, *Mater. Res. Soc. MRS Bull.*, *5*, 32–38.

Zundel, J. P., and B. Siffert (1985), Mécanisme de rétention de l'octylbenzene sulfonate de sodium sur les minéraux argileux, in *Solid-Liquid Interactions in Porous Media*, pp. 447–462, Technip, Paris.

P. Leroy and A. Revil, CNRS-CEREGE, Département d'Hydrogéophysique et Milieux Poreux, BP 80, F-13545 Aix-en-Provence, Cedex 4, France. (revil@cerege.fr)